# EFFECT OF BICEPS REATTACHMENT LOCATION ON MOMENT ARM

by

**David M. Weir**

B.S. in Mechanical Engineering, University of Pittsburgh, 2008

Submitted to the Graduate Faculty of

Swanson School of Engineering in partial fulfillment

of the requirements for the degree of

Master of Science in Mechanical Engineering

University of Pittsburgh

2010

UNIVERSITY OF PITTSBURGH

SWANSON SCHOOL OF ENGINEERING

This thesis was presented

by

**David M. Weir**

It was defended on

March 30, 2010

and approved by:

William W. Clark, Ph.D.,Associate Professor, Department of Mechanical Engineering and Material Science

Patrick Smolinski, Ph.D., Associate Professor, Department of Mechanical Engineering and Material Science

Mark Carl Miller, Ph.D., Associate Research Professor, Department of Mechanical Engineering and Material Science

Thesis Advisor: Mark Carl Miller, Ph.D., Associate Research Professor, Department of Mechanical Engineering and Material Science

**EFFECT OF BICEPS REATTACHMENT LOCATION ON MOMENT ARM**

David M. Weir, M.S.

University of Pittsburgh, 2010

The ultimate goal of the project is to quantify the effect of biceps tendon attachment location in clinically relevant terms, range of motion and torque generating ability as measured by muscle moment arm. Our hypothesis was that an anatomic repair would recreate native tendon moment arm and forearm rotation, while a non-anatomic insertion would compromise moment arm and forearm rotation.

Isometric supination torque and range of motion were measured for the native distal biceps tendon and 4 systematically placed repair points in 6 cadaveric specimens. A computer controlled elbow simulator, which exerts known loads on the forearm applied through the biceps tendon, was adapted to a device capable of measuring isometric forearm torque generated by cadaveric elbows.

For torque testing, the biceps tendon was loaded, and the torque generated was measured with the forearm fixed at 60° pronation, neutral, and 60° supination. Range of motion testing was done by incrementally loading the biceps while measuring the supination motion generated using a digital goniometer.

Tendon location and forearm position significantly affected the moment arm of the biceps. The native tendon had a mean moment arm of 5.67±2.86 and 10.44±1.45 (mm) in 60°

supination and neutral respectively. Anatomic repair in all forearm positions showed no significant difference from the native insertion. However, a centralized anterior repair was significantly lower in supination (0.15 ±3.48) and neutral (7.65 ±1.95) and also produced significantly less supination motion. No difference was observed between all tendon locations in pronation.

Clinically, these findings would suggest that patients with a biceps repair might experience the most weakness in a supinated position without experiencing a deficit in the pronated forearm. Surgically, particular attention needs to be paid to the geometry of the tuberosity and location of tendon reattachment as it could play a critical role in maximizing the functional outcomes of patients. The results of this study could help surgeons gain a better understanding of how to optimize their repair and thereby improve the expected outcome of their patients with distal biceps injuries.

## TABLE OF CONTENTS

## LIST OF FIGURES

# 1.0 INTRODUCTION

## 1.1 MOTIVATION

Avulsion of the distal biceps tendon from the tuberosity occurs mostly in middle-aged males resulting from eccentric loading of the flexed, supinated forearm [1]. When non-operative treatment is chosen, supination strength decreases by 50% and flexion strength is reduced by 35-40% [2]. Surgical repair has been shown to be a better alternative than non-operative treatments for restoration of strength and endurance [2, 3].

Current surgical methods include one and two incision repair techniques in which the tendon is reattached to the anterior or posterior aspect of the tuberosity respectively. Methods of attachment of the tendon include the use of sutures, suture anchors and cortical buttons. Although studies have examined the fixation strength of these types of repairs, little has been done to examine the effect of attachment location on functional outcome of the repair.

## 1.2 GOALS

The ultimate goal of the project is to quantify the effect of attachment location in clinically relevant terms, range of motion and torque generating ability as measured by muscle moment arm. The results of this study could help surgeons gain a better understanding of how to optimize their repair and thereby improve the expected outcome of their patients with distal biceps injuries.

# 2.0 BACKGROUND

The following section provides explanatory information on the anatomical and medical terms used throughout this thesis.

## 2.1 ANATOMIC DEFINITION

Because the human body can be placed into any number of positions, a standard reference configuration helps eliminate ambiguity when describing anatomical locations and features. All medical nomenclature is based on what is known as the anatomical position. In this position, the human body is standing with the arms hanging at the side, while the head and palms face forward as shown in Figure 1.

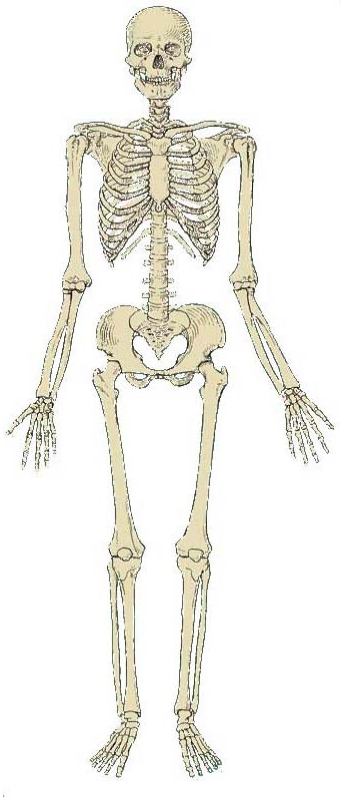

**Figure 1.** Human skeleton in anatomical position [4]

The anatomic directions are defined in relation to the anatomical position. The terms anterior and posterior are used to describe the front and back sides of the body. For instance, the palms face anteriorly in the anatomical position. Medial and lateral describe an objects position in relation to the vertical midline of the body. The ears are lateral to the eyes because they are further from the midline of the body. Structures that are further from the torso of the body are described as distal, while proximal describes structures closer to the trunk. For example, the elbow is proximal to the hand, but distal to the shoulder. Lastly, superior and inferior describes a structure's relation to the head. The knee is superior to the feet because the knee is above the foot.

Three common reference planes are associated with the human anatomical position. The transverse or axial plane horizontally divides superior and inferior portions of the body. The

coronal or frontal plane divides anterior and posterior cross sections. Sagittal planes separate medial and lateral sections of the body. These planes are illustrated in Figure 2.

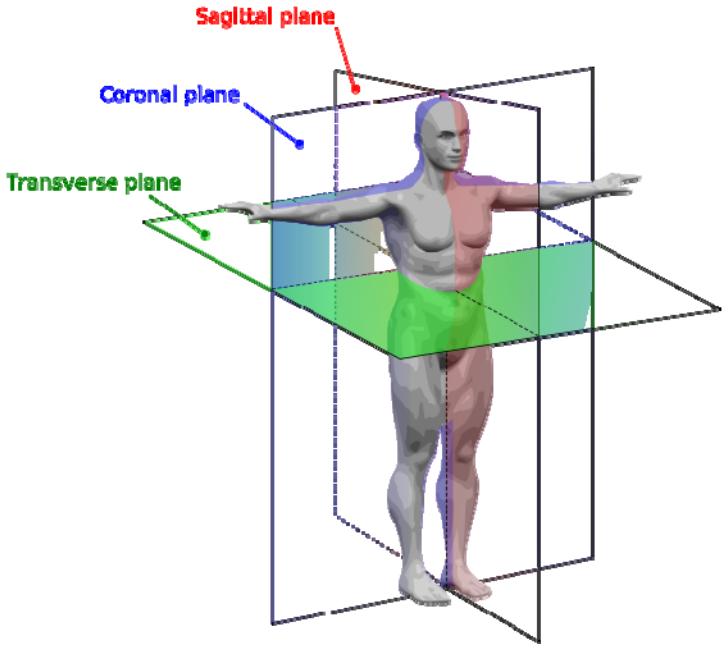


**Figure 2.** Illustration of anatomic reference planes [5]

## 2.2 ELBOW OVERVIEW

The anatomical focus of this research is the upper extremity, specifically the elbow and forearm complex. The radius, ulna, and humerus are the three bones that make up this complex. The radius is located on the lateral (thumb) side of the forearm and is easily identified by the cylindrically shaped proximal head. The ulna is located on the medial side of the forearm. The humerus is the long bone of the upper arm with the proximal end serving as the ball joint of the shoulder. Figure 3 shows the location of each bone for further reference.


**Figure 3**. Bones and joints of the forearm complex [6]

These three bones make up four joints allowing two types of motion. The radius and ulna form two articulations, the proximal and distal radioulnar joints. These joints allow for rotation of the radius around the ulna. This motion turns the palm anteriorly (palm up) or posteriorly (palm down), positions which are defined as supination and pronation respectively. As illustrated in the Figure 4, neutral forearm rotation is defined as 0°.

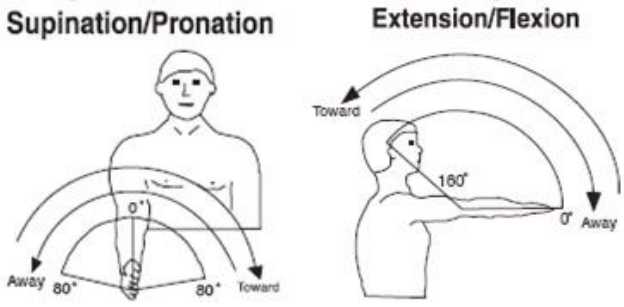


**Figure 4.** Angle conventions to describe forearm motion [7]

The radius and ulna each form an articulation with the humerus. The proximal end of the ulna forms a large concave bony process known as the trochlear notch. The notch fits in a groove of the cylindrically shaped process on the distal humerus called the trochlea. The head of the radius is cup shaped and articulates with the rounded ball shaped process on the distal humerus called the capitulum. These joints allow the angle between the humerus and forearm to decrease (flexion) or increase (extension). For flexion/extension, the fully extended arm is the 0° reference as illustrated in Figure 4. Figure 5 shows the locations of the different bony structures of the radius, ulna, and humerus.

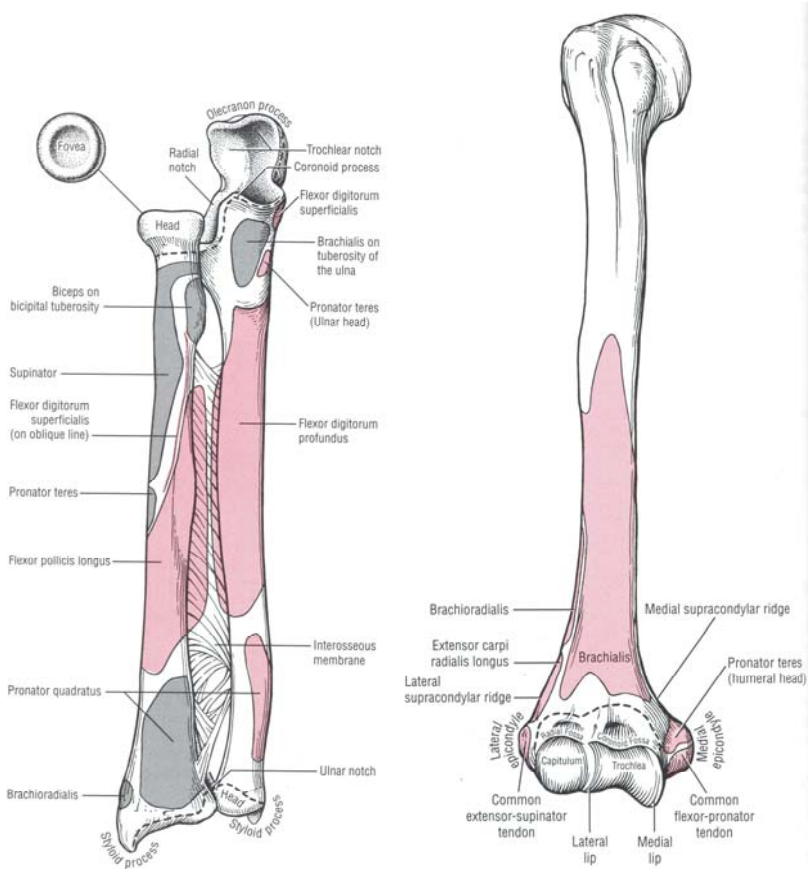


**Figure 5.** Bony structures and muscle attachments of the forearm (anterior view) [6]

Numerous muscles are involved in powering the motion of the elbow. Based on the motion that the muscle force facilitates, a muscle can serve as a flexor, extensor, supinator, or pronator. The main elbow flexors are the brachialis, biceps brachii, brachioradialis, and pronator teres. The triceps brachii and anconeus provide force for elbow extension. Forearm supination is powered by the biceps brachii and the supinator muscle, while the pronator quadratus and pronator teres power pronation. Figures 6 and 7 illustrate the location of each muscle.

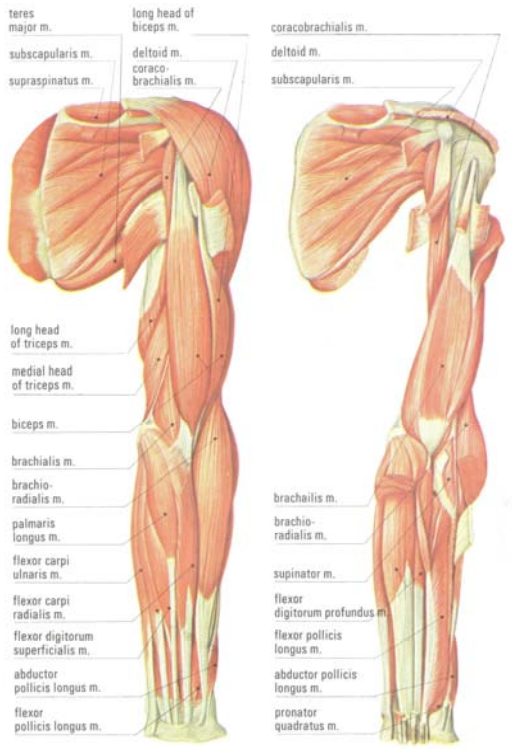


**Figure 6.** Location of forearm muscles (Anterior view) [8]

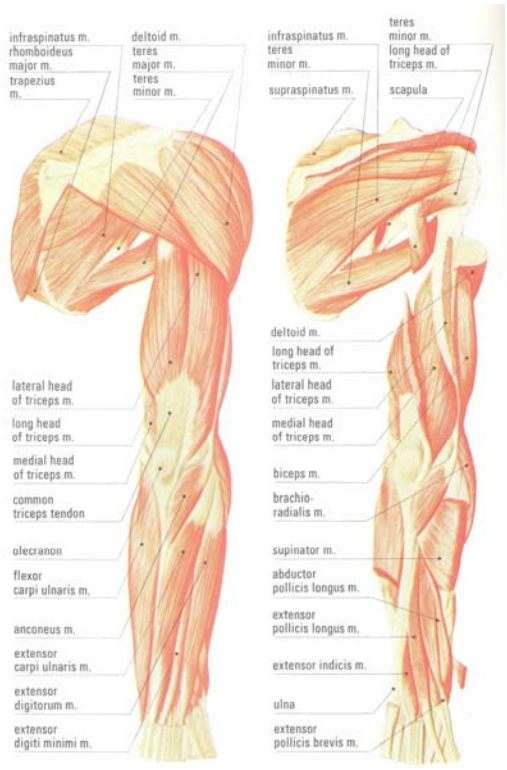


**Figure 7.** Location of forearm muscles (Posterior View) [8]

## 2.3 BICEPS BRACHII

As mentioned above, the biceps brachii muscle functions as an elbow flexor and as the dominant supinator of the forearm. Proximally, the biceps originates from two points, the supraglenoid tubercle and the coracoid process of the scapula. The distal biceps tendon inserts onto the radial (bicipital) tuberosity as shown in Figure 5. The radial tuberosity is a crescent shaped bony protrusion on the medial side of the proximal radius. The tendon inserts on the posterior ulnar side of the tuberosity. The distal biceps tendon rotates the radius about the ulna around an axis that extends through the center of the radial head and ulnar head. Figure 8 shows the position of the radius as the arm supinates.

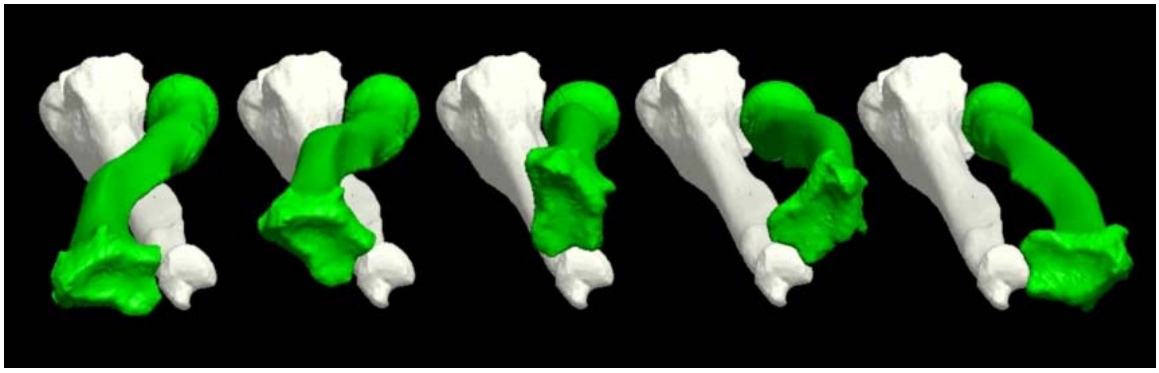

**Figure 8.** Rotation of the radius (green) around the ulna during supination

As the forearm pronates, the distal biceps tendon wraps around the tuberosity creating a cam-like effect. The added height of the tuberosity compared to the shaft of the radius is thought to place the biceps tendon in a more efficient position to supinate the forearm [9].

## 2.4 DISTAL BICEPS RUPTURES

The rupture of the distal biceps tendon is a relatively uncommon injury occurring only in 1.2 of 100,000 patients [10]. The injury usually occurs in the dominant arm of 40-50 year old males from eccentric loading of the supinated forearm such as during lifting activities [10-12]. Most patients note a single traumatic event followed by pain that gradually subsides.


**Figure 9.** Illustration of a distal biceps rupture [13]

During complete tears, a deformity in the biceps contour could occur [14]. Patients usually present with swelling of the forearm along with weakness in supination [11]. Smoking has been found to increase the risk of distal biceps rupture by nearly 8% [10]. Additionally, mechanical impingement could possibly contribute to the occurrence of rupture. It has been shown that the space between the radial tuberosity and ulna border decreases by 50% from full supination to full pronation [15].

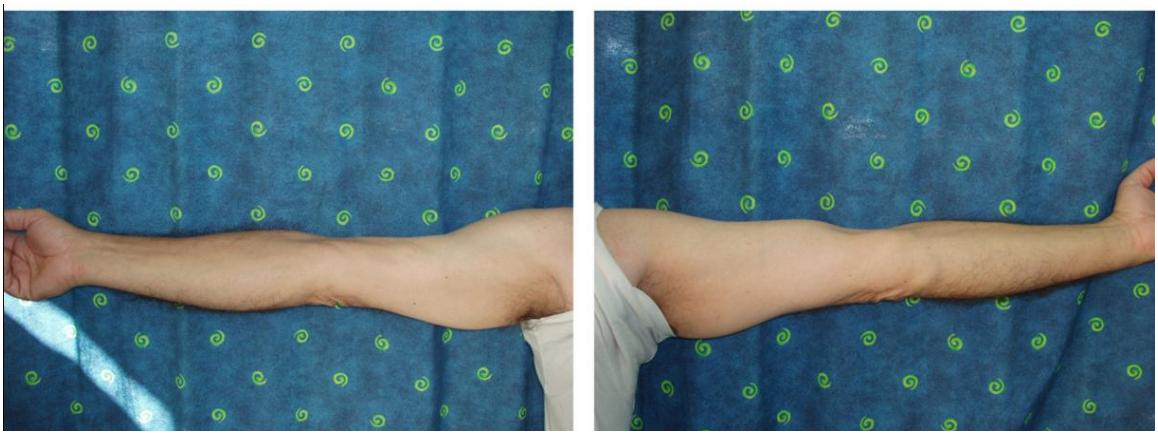

**Figure 10**. Deformity after rupture of right biceps treated non-operatively (Left). Normal contra lateral side (Right).[2]

## 2.5 SURGICAL TREATMENT OVERVIEW

The surgical treatment of the ruptured distal biceps tendon has evolved over the past century. Early surgical attempts to reinsert the biceps tendon to the radial tuberosity using an anterior approach were met with numerous complications[16, 17]. In 1941, Dobbie concluded that an anterior approach was "impractical and unwise" due to the numerous nervous and vascular structures of the proximal forearm near the tuberosity [16]. For this reason, some physicians opted for a simplified non-anatomic repair of suturing the biceps tendon to the brachialis [16, 17]. In 1960, Boyd and Anderson developed a two incision approach for reinserting the biceps tendon to the tuberosity as an alternative to the anterior approach [18]. In this approach, using a limited anterior incision, the tendon is passed between the ulna and radius while the forearm is pronated as shown in Figure 11.

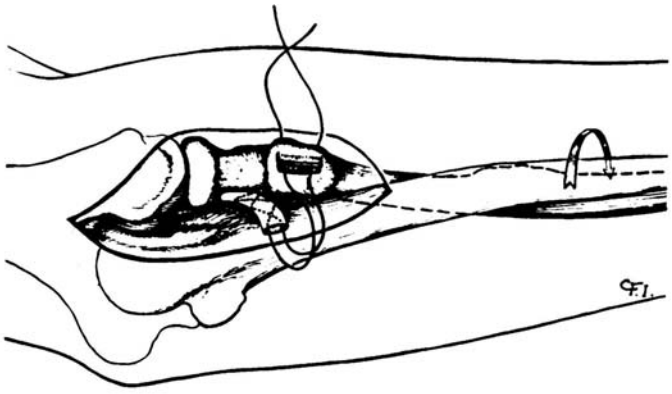

**Figure 11.** Biceps tendon passed between ulna and radius during Boyd Anderson approach.[18]

A second incision along posterolateral aspect of the elbow exposes the tuberosity for reattachment. The tendon is passed through a bone flap made on the tuberosity and sutured into

place. Boyd and Anderson claimed that this repair was safer and would restore the biceps as a dominant supinator of the forearm, unlike the brachialis attachment method [18].

With the advent of modern testing equipment to objectively evaluate patient strength, the efficacy of the different biceps repair techniques could be evaluated. In 1985, Morrey had one patient that was treated with the brachialis attachment method. Testing showed that the repair resulted in a 50% loss in supination strength [12]. Years later, others would report the same deficiency in supination using this method [19, 20]. These findings confirmed the claim made by Boyd and Anderson over twenty years earlier and provided further cause for anatomic repair. Baker and Bierwagen had a series of thirteen patients, three of whom were treated nonoperatively, undergo follow-up isokinetic muscle testing. Their study concluded that the Boyd-Anderson technique produced satisfactory results in returning normal elbow function to the patient, while conservative treatment led to weakness in strength and endurance [3]. Others have also shown similar results using the Boyd-Anderson technique by way of isokinetic testing [21].

However, the Boyd-Anderson technique was not without complications. Numerous studies reported cases of radioulnar synostosis, which is the fusion of the proximal radioulnar joint inhibiting forearm rotation as shown in the x-ray image of Figure 12 [12, 22-24].

**Figure 12.** Radiograph of proximal synostosis of forearm [22]

Failla en al. reported 4 cases of proximal radioulnar synostosis in patients who underwent the two incision technique. They concluded that the Boyd-Anderson has the potential to cause damage to the interosseous membrane, a hemotoma between the radius and ulna, or stimulation of the ulnar periosteum resulting in synostosis formation [22]. The authors suggested use of a modified Boyd-Anderson technique developed by Morrey utilizing a limited muscle splitting approach without exposing the ulna [12, 22].

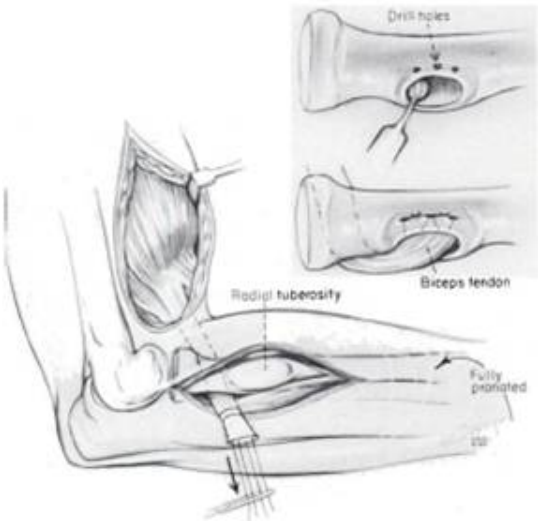


**Figure 13.** Modified Boyd-Anderson technique [12]

In a series of 74 patients, Kelly reported no instances of radioulnar synostosis using this modified Boyd-Anderson technique [25]. This approach was shown to produce satisfactory results in both dominant and non-dominant arms [11]. However in more recent literature, Bisson reported a higher complication rate (27%) including 3 cases of radioulnar synostosis (7%) using the modified Boyd-Anderson [26].

In 1993, Barnes published a method for reattachment of the tendon using Mitek anchors and a one incision anterior approach. The 4 patients in the series had satisfactory outcomes with no complications. Barnes attributed the lack of complications to the minimal exposure and drilling needed to place the anchors [27]. Le Heuc (1996), Balabaud (2004), and Kahn (2008) were able to produce satisfactory results using this technique, which provided further evidence in favor of minimally invasive anterior approaches [19, 28, 29].

In 1998, Strauch published a technique that used 2.5 mm Statak suture anchors with a single zigzag anterior incision [30]. Lynch later had successful outcomes by combining the Boyd-Anderson technique with Mitek suture anchor fixation [31].

In 2000, Pinto published a paper advocating the use of a single incision anterior technique [32]. That same year, Bain adapted the Endobutton fixation used in ACL reconstruction to a single incision anterior technique for distal biceps repair [33]. The technique provided strong fixation to allow for early mobilization, while simplifying the fixation method for the surgeon [34]. The Endobutton procedure has been shown by many published studies to produce satisfactory results [35-37].

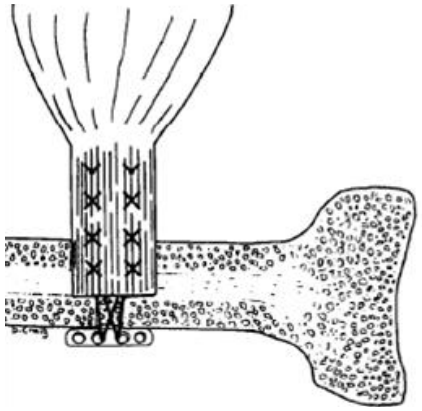

**Figure 14.** Bain's biceps fixation with Endobutton [33]

With many types of tendon anchoring devices in use, distal biceps research shifted towards biomechanical evaluations of the fixation strength of the repair. Early studies found that bone bridge fixation was stronger and stiffer compared to suture anchors [38]. However, these findings were contradicted in later studies. In 2003, Greenberg et al conducted a cadaveric study that tested three anchoring methods: Mitek Superanchor, conventional bone bridge, and the Endobutton. The Endobutton was found to provide the greatest pull out strength followed by the Mitek anchors [34]. Lemos compared the strength of bone bridge and Mitek anchors and found that the Mitek anchors were superior [39]. Idler compared the bone bridge and interference screw techniques. They found that the interference screws provided equivalent strength to the native tendon [40]. In 2006, Spang directly compared the Endobutton to suture anchors. The results of the study indicated that the Endobutton did not have statistically significant biomechanical advantages over suture anchors [41]. In a study that compared 13 different fixation methods, the Endobutton was found to have the highest load to failure, but noted that all fixation methods provided adequate strength [42]. Similar results were found in other studies that compared the Endobutton to other fixation methods [43, 44].

## 2.6 PREVIOUS WORK ON BICEPS MOMENT ARM

A muscle's moment arm can be used as a measure of the torque generating ability of a particular muscle about a joint. Numerous studies have shown that the moment arm changes with joint angle. In 1995, Murray showed that the moment arms of the major elbow muscles of both a male and female cadaver varied as a function of elbow flexion angle and forearm rotation angle. In this study, the moment arms were derived by taking the derivative of the 3$^{rd}$ order polynomial best fit curve of the tendon displacement and joint angle data. For the biceps, their testing showed the maximum moment arm (≈ 11 mm) occurred at approximately neutral with the arm flexed to 85° [45].

In 2001, Haugstvedt used a dynamic simulator to load the supinators and pronators of the forearm. The simulator included a torque sensor, positional sensors, and pneumatic actuators for muscle loading. With the elbow fixed at 90° of flexion, each muscle was ramp loaded while the torque generated was recorded. Each muscle was tested in 10° increments over the full forearm range of motion. The moment arm at each forearm position was calculated from the slope of the torque vs. load relationship. Their results showed that the biceps is the dominant supinator with a maximum moment arm occurring in a slightly pronated position [46]. Figure 15 shows a plot of the results.

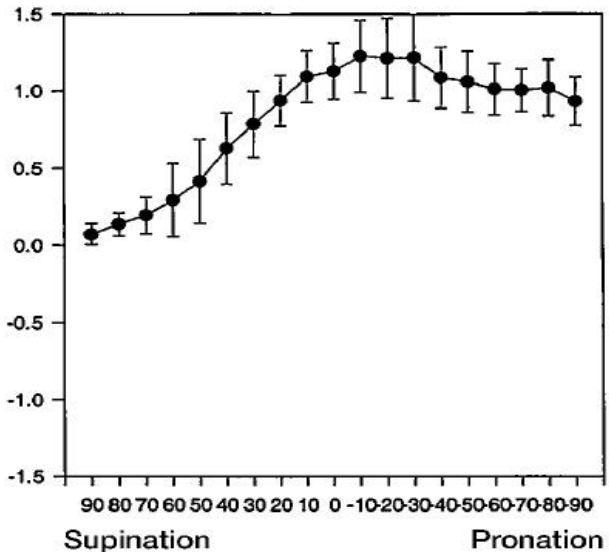


**Figure 15.** Moment arm (cm) data from Haugstevdt. [46]

## 2.7 PREVIOUS WORK ON THE EFFECT OF ATTACHMENT LOCATIONS

Only one study was identified in the medical literature that tried to examine the effect that reattachment location has on the biceps [47]. Henry et al used a static weight (100 N) to load the biceps and measured the supination force generated in pairs of matched cadaveric elbows with a load cell. The elbow was fixed a 90° of flexion and one end of a ¼" pin was placed in the distal radius. The other end of the pin was placed parallel to an axial load cell to measure the resultant force when the biceps was loaded. The native tendon was tested first as a baseline. Then the distal biceps was transected and tested after repair using an anterior attachment site on the tuberosity. In the contra lateral arm, the testing was repeated using a posterior attachment site.

Their data showed that there was no significant difference in the supination force generated between the anterior and posterior insertions. However, the study had several limitations that need to be considered. First, one major limitation was that the cadaveric elbows

were only tested in neutral rotation, so the behavior throughout the range of motion is unknown. Second, torque was not measured directly. The torque values reported were derived quantities based on the length of the pin. The study did not mention any systematic identification of the attachment sites across all the specimens leaving very little anatomic insight to the orthopaedic surgeon. Lastly, the surgical techniques required some burring of the tuberosity, which may have significantly altered the geometry of the radial tuberosity. This limitation narrows the focus of the study down to a comparison between two surgical techniques as opposed to a more in depth biomechanical analysis of insertion site location.

# 3.0 PRELIMINARY ANALYSIS

Because of the limited information in the literature, there is little understanding to the effect of tendon attachment location on the biceps. Due to the availability and cost of cadaveric specimens, it was important to try to estimate the effect size to examine whether it could possibly have clinical significance before starting biomechanical testing. A preliminary analysis was conducted to estimate the bicep supination moment arm of varying attachment locations over the range of motion of the forearm. This was achieved by using spatial data from Magnetic Resonance Imaging (MRI) to create a virtual model of the radius and calculating the moment arm at discrete angles in a matlab based simulation.

## 3.1 MRI IMAGING

The author of this thesis voluntarily underwent MRI imaging of the right forearm. Imaging of the distal biceps was done using the flexed abducted supinated (FABS) view as described by Giuffrè and Moss [48]. In this position, the person lies on their stomach with the fully supinated arm flexed to 90° and placed above the head. Sand bags were used to help stabilize the arm and prevent movement during imaging. Sequences of images of the forearm were taken in the coronal and sagittal views.

## 3.2 DICOM

MRI images are saved in a Digital Imaging and Communications in Medicine (DICOM) file format. This format provides a set of standards for the information contained in a medical image. Manufacturers of imaging equipment provide a certificate of DICOM compliance for their equipment. Embedded in the attributes of the file is key information regarding patient information, image position, and pixel settings. These attributes allow for the spatial mapping of pixels in a DICOM image.

## 3.3 PREPROCESSING

The MRI images were imported into Mimics software (Materialise, Leuven, Belgium). Mimics allows the user to process 2D image data and reconstruct accurate 3D models of the data. Mimics was primarily used for extracting points on bone surface geometry as well as key anatomic points. Using the segmentation and curve fitting tools, a sliced point cloud of pixels representing the surface of the proximal radius was created. The centerline tool was used to define the pixels at the center of radial head and center of ulnar head. Pixels were also chosen to represent different possible insertion points of the distal bicep tendon. The pixel and image data was then exported as a text file and imported into a formatted excel spreadsheet to allow for processing in Matlab R2009a (MathWorks, Natick, Massachusetts). The pixel data was loaded into a Matlab program that spatially maps each pixel following the transformation provided in PS 3.3 2007 of the DICOM Standards and outputs a dataset of xyz coordinates. The details of the program can found in Appendix A.

## 3.4 SIMULATION

The spatial data for points on the surface of the proximal radius and anatomic key points were loaded into the Matlab simulation program. The program defines the axis of forearm rotation by the vector connecting the center of radial head and the center of the ulnar head. The origin of the tendon is also estimated from the length of the humerus. The surface points of the radius are oriented and meshed in a fully supinated position (-80°) around the forearm axis and plotted for visualization.

Next, the user specifies the coordinates of a specific point to represent the insertion location. The line of action of the biceps force is determined by the vector connecting the tendon insertion to the tendon origin. Logic based on a vector direction comparison is implemented to determine whether the tendon is wrapped around the radius at the current orientation. If wrapping occurs, a contact point that is limited to the plane of the insertion slice is calculated and used to determine the correct force vector direction. The cross product of the force vector about the center of the radial head is first computed. To find the moment arm, the dot product of this result with the axis of forearm rotation unit vector is calculated. Finally, all of the spatial points are rotated in 10° increments about of the forearm axis and the calculation cycle is repeated until the radius is fully pronated (80°). The program outputs a file containing the forearm position and corresponding estimate for the biceps supination moment arm. The details of the program code can be found in Appendix B.

## 3.5 RESULTS

Figure 16 shows the moment arm estimates vs. forearm position curves for five different insertion locations. The results show that as the insertion is moved lateral on the anterior radius, the supination moment arm was lower while in the supinated forearm. However, as the arm pronates, the moment arms were equivalent for all repairs. According to these estimates, moving the insertion anterior can create up to a 25% loss in moment arm. The orthopaedic surgeons collaborating on this project concluded that a loss of this size could potentially be clinically relevant especially in biceps repaired using an anterior approach. Based on these estimates, it was decided to proceed with a cadaveric biomechanical study.

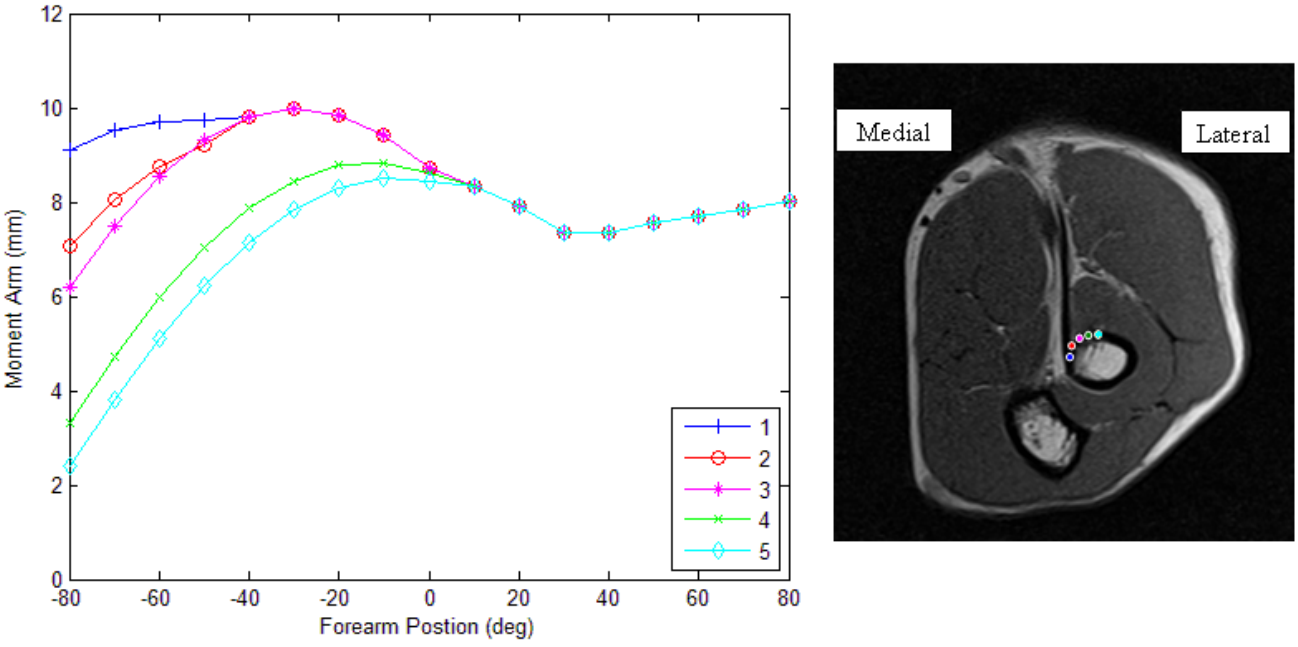


**Figure 16.** Moment arm estimates vs. forearm position curves for five different insertion locations

# 4.0 METHODS

## 4.1 PROJECT OVERVIEW

Isometric supination torque and range of motion were measured using 6 cadaveric specimens. The specimens were mounted in an elbow simulator, which consisted of a computer controlled linear actuator to exert known bicep loads. For torque testing, the forearm was rotated and locked into three positions: 60° pronation, neutral and 60° supination. The biceps tendon was loaded, and the torque generated was measured with an attached sensor for the native tendon attachment. The tendon insertion site was then transected, reattached, and tested at 4 different locations. The torque vs. load data was plotted to determine the bicep moment arm for each tendon attachment. Range of motion testing was performed by unlocking the radius and incrementally loading the biceps. The forearm motion for the native tendon and each location was measured using a digital goniometer. A two-way repeated measures analysis of variance with Tukey's post-hoc testing was used for statistical analysis.

## 4.2 CADAVERIC SPECIMENS

A total of 6 frozen upper extremity cadaveric specimens (5 male), with an average age of 60 (36-83) years, were used. The specimens included the full forearm from the hand to the mid-humerus proximally. Specimens with medical histories of rheumatoid arthritis, degenerative joint disease or any orthopaedic anomaly were excluded. One specimen was replaced because it

was unable to pronate past 30°. Prior to the day of testing, each specimen was allowed to thaw overnight at room temperature and kept moist with normal saline.

## 4.3 TESTING APPARATUS

### 4.3.1 AGH Elbow Simulator

A previously developed elbow simulator was used to provide reliable and consistent loading to the forearm muscles. The simulator included computer controlled linear actuators to exert known loads on the forearm applied through the muscle tendons. The tendons were connected to the actuators using a Krackow locking loop stitch (Figure 17) and 80 lb test line. These lines were then passed through pulleys to provide the proper line of action of the muscle force.

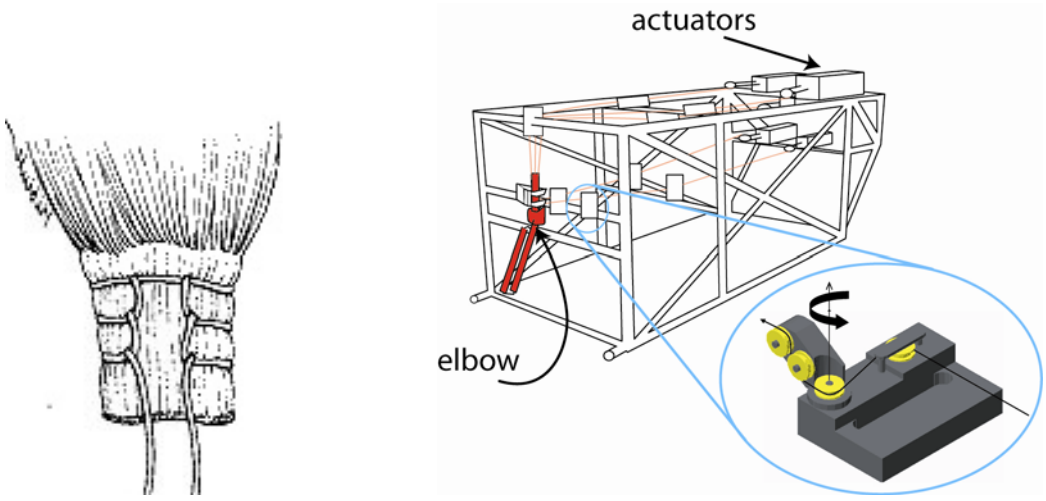


**Figure 17.** Drawing of Krackow locking loop stitch (left) and the AGH elbow simulator (right).

For this project, only the biceps actuator was activated. The controller operates on a proportional-integral-derivative feedback control and a new controller program was written

specifically for this project. The program sends a sinusoidal reference signal to the biceps actuator. For the first 100 samples, the reference signal was set to a constant 1 lb load to remove any slack from the system. For the next 600 samples, the input was a sinusoid with amplitude of 14 lbs. The last 100 samples returned the load to a constant 1 lb load. Figure 18 shows the graph of the resulting biceps load output.

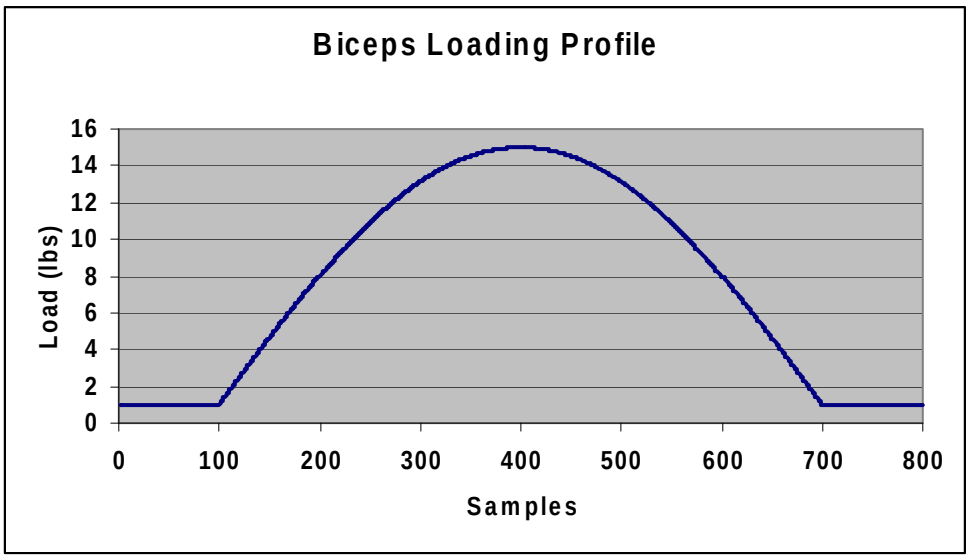


**Figure 18**. Biceps loading profile.

The 15 lb maximum bicep load was chosen based on data in the medical literature. Greenberg et al showed that the mean biceps force needed to flex 15 cadaver arms to 130° was 67 N (≈15 lbs) [34]. For this reason, 15 lbs was determined to be a reasonable approximation of the physiological loading that could occur. The entire code for the program is included in Appendix C.

### 4.3.2 Supination Torque Device

A device capable of measuring isometric forearm torque in cadaveric specimens was developed to attach to the existing elbow simulator assembly. During previous work on this device, an 80/20 aluminum channel with turnbuckle style support system was retrofit to the front of the elbow simulator frame as shown in Figure 19.

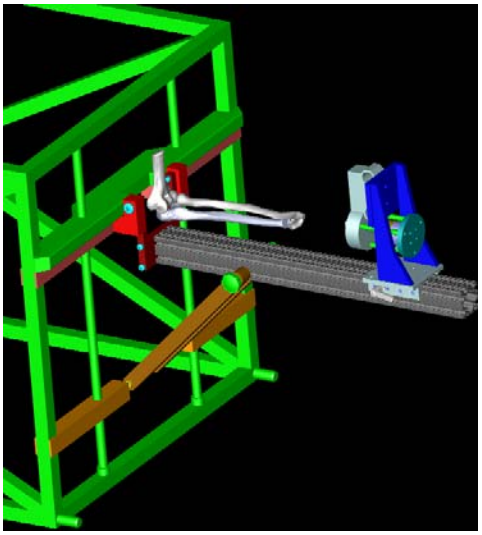

**Figure 19.** Existing support structure retrofit to elbow simulator.

The aluminum channel supported a carriage with a torque sensor that could translate and lock into place. To align the sensor with the forearm axis of rotation, an additional piece of aluminum channel was mounted perpendicularly to the first channel. Also, a shoulder bolt was placed through the center of the carriage plate to allow for rotation.

To transmit the supination torque of the forearm, a torsional load transfer plate with a slot machined through the center was bolted to the torque sensor. A flat was machined into a shaft such that it would fit into the transfer plate slot. Next, an aluminum friction clamp attached to the load cell shaft. The friction clamp allowed the assembly to rotate and lock into different

positions about the load cell axis. An aluminum plate with a pattern of holes was fabricated such that it could be bolted to the distal radius. Next an adjustable shaft with a universal joint was used to connect the plate to the load cell shaft clamp. The final assembly allowed the forearm to rotate and lock into different supination/pronation angles and it offered enough flexibility and adjustment to handle the natural variability found among cadaveric specimens.

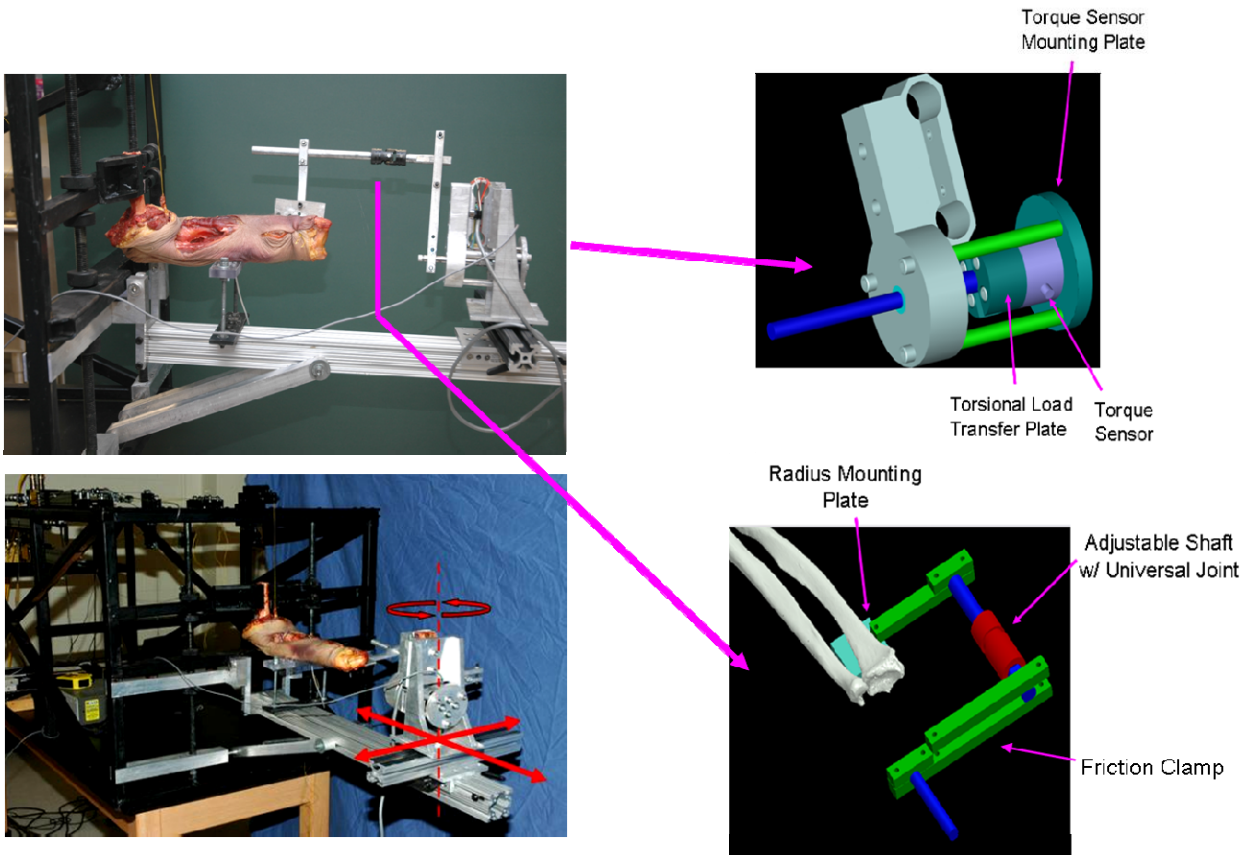


**Figure 20.** Final assembly of testing apparatus.

## 4.4 DATA ACQUISITION SETUP

To determine the moment arm, the torque and biceps load data needed to be captured simultaneously. The torque sensor and biceps load cell outputs were connected to an NI-6008USB A/D converter. The sample rate for the A/D converter was set to 60 Hz to match the sample rate of the torque sensor signal conditioner. The converter was connected to a separate laptop with Matlab R2008a. A program was written in Matlab to acquire the data and to provide real-time plotting of the supination torque and biceps load during testing. A copy of the code can be found in Appendix D.

## 4.5 TORQUE TEST PROTOCOL

Each specimen was mounted in the elbow simulator with the humerus and ulna fixed firmly to the frame at 90° of flexion. The proximal end of the distal biceps tendon was attached to an actuator using 80 lb test line. The adjustable shaft was attached to the distal radius plate. The forearm was then rotated and locked into each of three positions: 60° supination, neutral and 60° pronation. The biceps tendon was loaded to 66.75 N (15 lbs), and the torque was measured for the native tendon attachment. The distal biceps tendon was transected, and surgically reattached using a cortical button and then tested at each of the four different locations. A modified cortical button fixation was well-suited for the tests because it did not compromise the radius bone of the specimen. Also, this type of fixation is the preferred method by the senior orthopaedic surgeon. For each forearm position, each test was repeated three times.

### 4.5.1 Tendon Attachment Locations

With the arm fully supinated, the borders of the radial tuberosity were identified, and the lines marking the proximal and distal border were drawn. The borders were defined at the points where the bone geometry of the radius begins to exhibit slight concave curvature. The length of the tuberosity borders was measured and their midpoints were marked. A line connecting the two midpoints defined the center axis line. The highest point (apex) on the tuberosity at the tendon-bone interface was identified using calipers. A medial to lateral line, parallel to the tuberosity border lines, was drawn to define the apex diameter line.

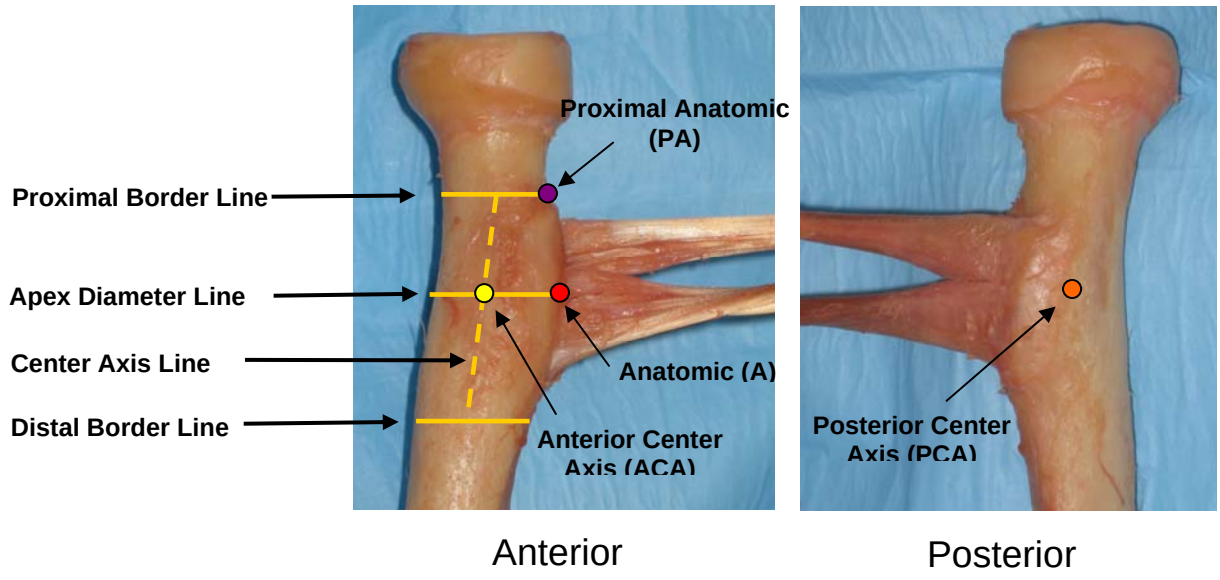


**Figure 21.** Diagram of distal biceps tendon reattachment locations.

Using these markings as a guide, three drill holes (2.25 mm diameter.) were systematically placed in the radius. Location anatomic (A) was placed on the apex diameter line at the native tendon insertion. Location anterior center axis (ACA) was drilled at the intersection of the center axis and apex diameter lines. Location posterior center axis (PCA) is the same as

anterior center axis except that the tendon wrapped around the tuberosity and attached on the posterior side of the radius. Location proximal anatomic (PA) was drilled at the most ulnar point on the proximal borderline. This systematic approach based on the radius geometry for identifying the insertion sites allowed for consistent placement across all specimens.

### 4.5.2 Mathematical Background

Mathematically, torque, $\vec{\tau}$ , is represented by the cross product of the force vector, $\vec{F}$ , and the position vector, $\vec{r}$ , shown in Equation 1.

$$\vec{\tau} = \vec{r} \times \vec{F} \qquad (1)$$

The position vector, $\vec{r}$ , is a vector from a point on the axis of interest to the point where the force is applied. By definition, the magnitude of the cross product of $\vec{r}$ and $\vec{F}$ can be written as:

$$\left|\vec{\tau}\right| = \left|\vec{r}\right| \cdot \left|\vec{F}\right| \cdot \sin\theta \qquad (2)$$

Where,

$\left|\vec{\tau}\right|$ =magnitude of the torque, $\vec{\tau}$

$\left|\vec{r}\right|$ =magnitude of the position vector, $\vec{r}$

$\left|\vec{F}\right|$ =magnitude of the force vector, $\vec{F}$

$\theta$ =angle between $\vec{r}$ and $\vec{F}$

The perpendicular distance between the moment axis and the line of action of the force defines the moment arm, $d$, and its magnitude is given by the $|\vec{r}| \cdot \sin\theta$ term in equation 2. By rearranging Equation 2, the moment arm can be calculated as shown by:

$$d = \frac{|\vec{\tau}|}{|\vec{F}|} = |\vec{r}| \cdot \sin\theta \qquad (3)$$

Mathematically, Equation 3 illustrates that one would expect a linear relationship since the distance from the axis, $|\vec{r}|$, and the angle $\theta$ remain constant at fixed forearm rotation positions. As it relates to supination torque, the only times these parameters can change is when either the forearm rotational position or the insertion site location is changed. Therefore, if the moment arm, $d$, remains constant, then the torque will have a direct relationship with the force, i.e. torque increases as force increases or vice versa, and will be scaled by a factor equal to the moment arm.

For this study, the magnitudes of the supination torque and biceps load were measured simultaneously. We tested all tendon attachment locations at the same forearm rotational positions under the same biceps muscle loading profile. By comparing the moment arms for each attachment location at a given forearm rotation position, the effect of the attachment location could be determined. Therefore, any change in the torque generated was due to a change in the muscle moment arm resulting from varying the attachment location.

A linear regression line was fitted to the supination torque vs. bicep load data for each torque test as shown by Figure 22. The moment arm for each tendon attachment was defined as the slope of the regression line. The moment arm was averaged over the three repeated tests taken at each forearm position. A positive moment arm value indicated that the biceps generated a supination torque.

## 4.6 SUPINATION MOTION TEST

The humerus and ulna were firmly fixed at 90° of flexion. The only degree of freedom allowed was forearm rotation. A line was drawn on the distal radioulnar joint (DRUJ) through the radial and ulnar styloids. This line was used to define the forearm's rotational position with a digital goniometer. It was hypothesized by the investigators that a more efficient attachment would supinate the arm more under the same load when compared to the others. With no load on the biceps tendon, the arm was placed in pronation. The biceps was then loaded incrementally from 0 N to 22.25 N (5 lbs), 44.50 N (10 lbs), and then 66.75 N (15 lbs), and the forearm position was measured. The test was repeated three times for each biceps tendon attachment location.

## 4.7 DATA ANALYSIS

### 4.7.1 Filtering Data

Supination torque and biceps load data were filtered using a lowpass Butterworth filter in Matlab. Filter parameters were adjusted until a smooth curve was achieved. The matlab code is included in Appendix E.

### 4.7.2 Statistical Methods – Torque Data

A linear regression line was fitted to the torque vs. load data for each test as shown by Figure 3. The moment arm for each tendon attachment was defined as the slope of the regression line. The

moment arm was averaged over the three tests taken at each position. A positive moment arm value indicated that the biceps generated a supination torque.

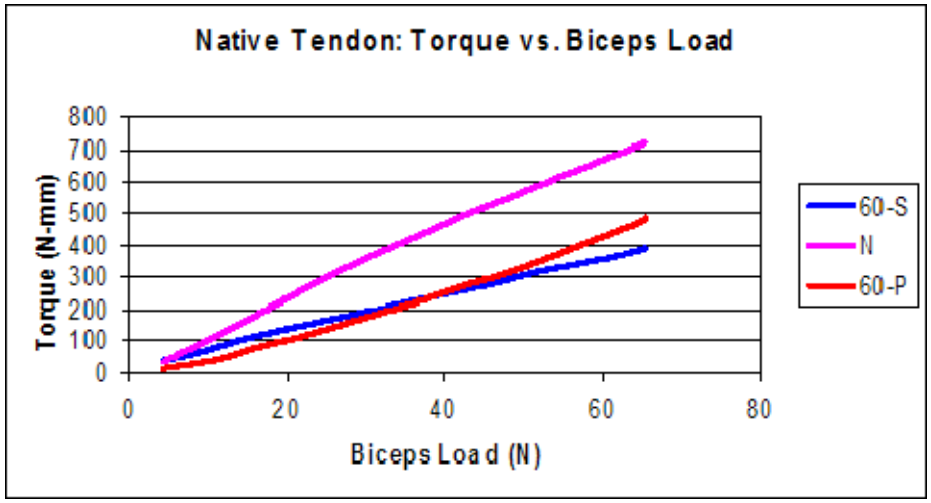


**Figure 22.** Example of torque vs. biceps load relationship for native tendon.

A two-way repeated measures analysis of variance was used to determine if tendon location and forearm position significantly affect the moment arm of the biceps ($p < 0.05$). Tukey's post-hoc testing was used to compare the means of individual treatment levels with one another.

### 4.7.3 Statistical Methods – Supination Motion Data

A two-way repeated measures analysis of variance was used to determine if tendon location and biceps load significantly affected the moment arm of the biceps ($p < 0.05$). Tukey's post-hoc testing was used to compare the means of individual treatment levels with one another.

# 5.0 RESULTS

## 5.1 GROSS OBSERVATIONS

The native biceps tendon appeared to insert normally in all specimens. Each native tendon inserted slightly posterior of the most ulnar edge of the tuberosity in a ribbon-like fashion. At 60° supination, minimal wrapping of the tendon around the apex of the tuberosity was observed. As the forearm was pronated, an increase in tendon wrapping was observed with definitive wrapping occurring just before neutral. Location anatomic exhibited a similar wrapping behavior.

For location anterior center axis, minimal tendon wrapping was observed at all three forearm positions due to the centralized placement of the repair. Slight wrapping may have occurred at near full pronation of the forearm which is a comparably larger angle than observed in the native case.

For posterior center axis, tendon wrapping was observed at all three forearm positions. At this location, the tendon was acting over the apex of the tuberosity at all times.

For the proximal anatomic location, minimal wrapping occurred at 60° supination. As the forearm pronated, the tendon wrapped around the proximal junction of the tuberosity and radial shaft.

## 5.2 MOMENT ARM RESULTS

Analysis showed that tendon location and forearm position significantly affected the moment arm of the biceps ($p<0.05$). The native tendon had a mean moment arm of 5.67 ±2.86, 10.44 ±1.45 and 8.04 ± 1.25 (mm) in 60° supination, neutral and 60° pronation respectively. Our native tendon moment arm data compares well with other findings published in the medical literature which provides some validity to the methods used [45, 46]. Murray et al reported an estimate of 13 mm for the biceps moment arm of males at neutral. From the plots published by Haugstvedt, the average moment arms were approximately 2.5, 11, 10 mm for 60° supinated, neutral, and 60° pronated respectively. This data is comparable to the average native moment arm values of 5.7, 10.4, and 8.0 mm found in this study.

Reattachment to an anatomic location in all forearm positions respectively (6.24 ±3.30, 10.41±2.03, 8.41±1.22) showed no significant difference from the native insertion. Location anterior center axis had a moment arm which was significantly lower in supination (0.15 ±3.48) and neutral (7.65 ±1.95) compared to the native insertion, while no difference was found in pronation (8.26 ±1.88). In two specimens, this position created a pronation torque at 60° of forearm supination.

Location posterior center axis was significantly higher in supination (7.21± 3.02) compared to the native, however no differences were found in neutral and pronated positions.

Location proximal anatomic trended to have a lower moment arm than the native in all forearm positions, but was only significantly different in neutral (8.83±2.06). In supination, location proximal anatomic's moment arm was 4.69 ±2.75 which was significantly higher than location center axis. No difference was observed between all tendon locations in pronation.

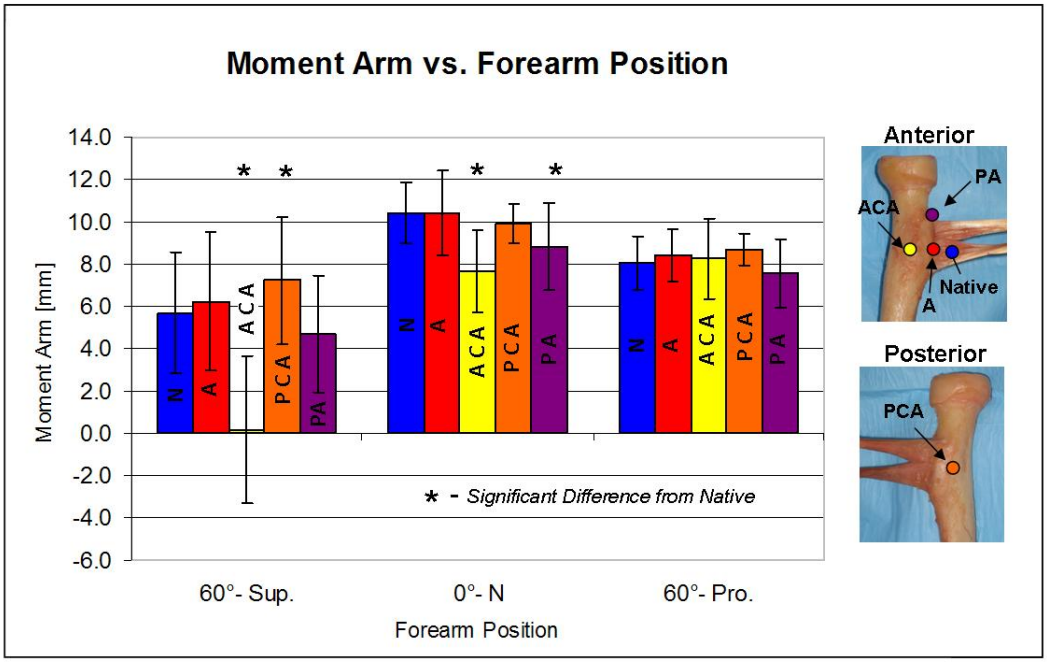


**Figure 23.** Summary of results for moment arm vs. forearm position.

All of the results are summarized in Figure 23 as well as in Appendix F.

## 5.3 SUPINATION MOTION RESULTS

Analysis showed that tendon location and biceps load significantly affected the supination motion of the biceps ($p<0.05$). The native tendon produced 68°±9°, 71°±9°, and 73°±10° of supination motion at 22.25 N, 44.50 N, and 66.75 N respectively. Location anatomic was not significantly different than the native tendon producing 70°±10°, 74°±10°, and 75°±11° at each level respectively. At 44.50 N, and 66.75 N, location anterior center axis was significantly lower than the native tendon (59°±17°, 62°±16°, and 62°±16°). No significant differences were found for the other locations. At 22.25 N, 44.50 N, and 66.75 N, location posterior center axis was significantly higher than the native tendon (74°±8°, 78°±8°, and 80°±8°). Location proximal

anatomic was not significantly different than the native tendon producing 68°±11°, 71°±10°, and 73°±9° at each level respectively.

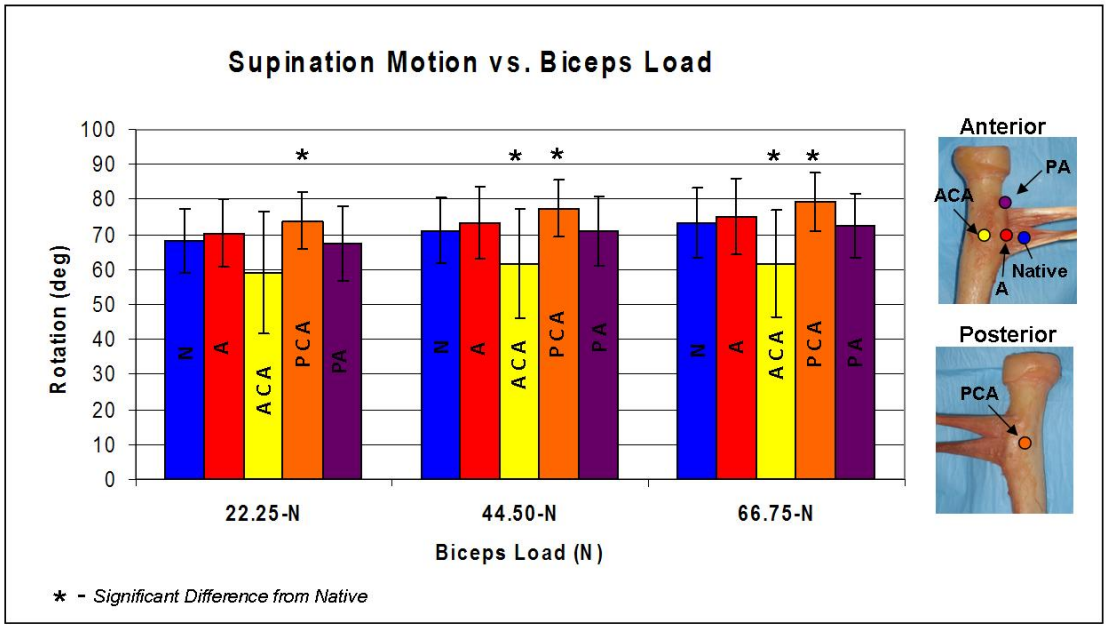


**Figure 24.** Summary of results for supination motion vs. biceps load.

All of the results are summarized in Figure 24 as well as in Appendix F.

# 6.0 DISCUSSION

The supination torque generated by the bicep tendon is a function of both the contractile force of the biceps muscle and the tendon's moment arm. During repair of ruptured distal bicep tendons, the surgeon's goal is to restore preinjury function. The patient's bicep muscle force is predetermined; however, this study showed that tendon reattachment location can influence supination moment arm by determining what portions of the radius the tendon wraps over during pronation.

Our native tendon moment arm data compares well with other findings published in the medical literature which provides some validity to the methods used [45, 46]. Murray et al reported an estimate of 13 mm for the biceps moment arm of males at neutral. From the plots published by Haugstvedt, the average moment arms were approximately 2.5, 11, 10 mm for 60° supinated, neutral, and 60° pronated respectively. This data is comparable to the average native moment arm values of 5.7, 10.4, and 8.0 mm found in this study.

The study showed that reattachment of the distal bicep tendon to its anatomic position showed no difference in moment arm to the native. Radializing the attachment, location anterior center axis, resulted in a significantly lower moment arm than the native in neutral (-27%) and supinated (-97%) positions with the greatest difference being in supination. We believe this observation is caused by the loss of the biceps tendon wrapping around the tuberosity**.** As the forearm pronates, the tendon can only wrap around anterior portions of the radius that are radial to the insertion site as shown by Figure 25**.** Therefore, for location anterior center axis, the tendon will never act over the added height of the tuberosity effectively reducing the moment

arm. Our data provides evidence that the radial tuberosity functions as a cam which improves the moment arm as has been suggested in the literature [47]. This finding is further supported by an increase in moment arm at the posterior center axis location with the arm in a supinated position. At this attachment location, the tendon wraps around the entire tuberosity throughout the full range of motion**.**

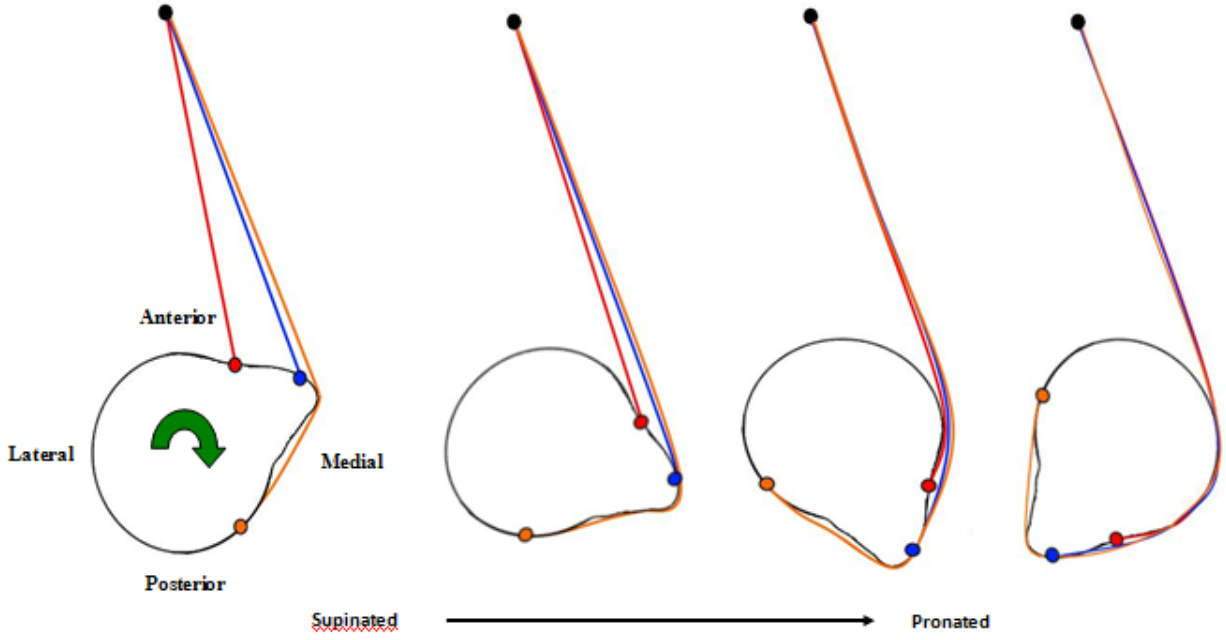


**Figure 25:** Illustration of tendon wrapping during pronation for various attachment locations. Left radius outline viewed from proximal to distal. Anterior repair (red), Anatomic Insertion (blue), and Posterior repair (orange).

We also observed that the biceps acted as a pronator at 60° supination for anterior center axis attachment location in two specimens. For this to occur, the biceps must apply a force to a point on the radius located on the radial side of the axis of forearm rotation. Compared to the native insertion, the anterior center axis insertion is positioned more radially on the anterior radius. In two specimens, this radial movement was sufficient to allow the insertion to cross to

the radial side of the forearm axis at 60° supination. However, as the forearm pronated, the insertion crosses back over to the ulnar side of the axes and acted as a supinator in neutral and 60° pronation.

Henry et al measured the resultant supination force generated by eleven pairs of cadaveric arms in neutral forearm position using both an anterior and posterior repair method [47]. For the anterior group, the biceps was sutured to the anterior tuberosity using a cortical bone bridge on the posterior tuberosity [49]. Posterior reattachment was done using the modified Boyd-Anderson approach [12]. An incision along posterolateral aspect of the elbow exposes the posterior tuberosity. The tendon is passed between the ulna and radius while the forearm is pronated, and a cortical window is burred into the tuberosity. The tendon is seated into the cavity and sutured into place using a bone bridge.

Their findings showed no significant difference between the two repairs. Some limitations of the study were that the arms were only tested in neutral and that muscle moment arms were not measured. Studies have shown that the biceps moment arm could change nonlinearly with forearm position making conclusions of the behavior throughout the entire range of motion difficult from one position. Also, both surgical techniques that were being compared required some burring of the tuberosity which may have significantly altered the geometry of the radial tuberosity making it difficult to isolate just the effect of attachment location alone.

The cortical button technique used in this study allowed examination of the effect of attachment location without drastically changing the native radius morphology and provided insight into the significance of the geometry. The effect of creating a cortical window in the tuberosity during a two incision Boyd-Anderson repair has been previously suggested to

decrease the moment arm due to tuberosity height reduction [9]. Our results support the importance of maintaining the tuberosity height and show that the ideal surgical repair for distal biceps ruptures would be one that required minimal alterations to geometry of the radius. This would allow the tendon to wrap over the apex of the tuberosity, and thereby in effect maximizing the muscle moment arm.

The study further showed that tendon location had no impact on the moment arm at 60° pronation. As the radius pronates, there is a certain point at which the tendon will begin to wrap around the radius. For each tendon location, this will happen at a different angle of forearm rotation. However, the angle when all of the tendon locations begin to experience wrapping, the moment arms should be almost equivalent. The tendon will be wrapping around the radial side of the radius which typically has small geometric variation over the length of the tuberosity. At 60° pronation, we believe this angle was surpassed resulting in no difference in moment arms across all locations. These findings could suggest that patients with a biceps repair might experience the most weakness in a supinated position without experiencing a deficit in supination strength in the pronated forearm.

Most of the strength testing in the literature has been done using commercial dynamometers for isokinetic testing of the biceps with comparisons of peak strength values usually defined as the maximal torque produced during the range of motion [2, 3, 11, 20, 23, 24, 28, 31, 50-57]. One study found that peak supination torque occurred at 12° of forearm supination during isokinetic testing of a normal population leading one to believe that the peak strength measurements in the literature might not be representative of the entire function of the repair [50]. One weakness of reports with isokinetic testing is that no comparisons are made on the supination strength differences of patients at different forearm positions other than positions

of maximum torque. For this type of muscle testing, it may be difficult to find isolated supination weakness due to the dynamic nature of the testing.

Some supination isometric testing of bicep patients has been reported, but patients are most commonly tested at neutral forearm rotation [12, 29, 56, 58-61]. Isometric testing has shown that after surgical repair, the injured arm regains 87%-93% of the supination strength of the uninjured arm [58-60]. However, our results suggest testing at more forearm positions especially in supination is warranted. We believe that a larger deficit is most likely to be found in the *supinated* forearm during isometric testing, especially in biceps repaired without restoration of the native insertion site. Based on previous supination strength testing protocols in the literature, the authors feel that a strength deficit in the *supinated* forearm might be under reported.

Historically, some literature has shown that patients with distal biceps ruptures may have reduced supination endurance ranging from 10-65% after repair [2, 20, 23, 24, 31, 52]. With a compromised supination moment arm, the patient would require greater muscle contraction to produce the same torque prior to injury which could provide an explanation to the reduced endurance that has been reported. The muscle moment arm is directly related to the mechanical advantage of the muscle. In other terms, this means that the larger the moment arm, the higher the efficiency of the muscle i.e. produces more output for a given input**.** Based on our findings, a patient with an anterior center axis repair could potentially have decreased supination endurance as well as peak torque due to the reduction in moment arm.

We hypothesized that the effect of tendon location would show up not only in comparing the moment arms directly, but also in comparing the amount of supination motion generated by the cadavers for a given biceps loads. The higher the moment arm, the more supination motion

we expected it to generate. The findings from our supination motion test confirmed that location anterior center axis is at a mechanical disadvantage compared to the other locations i.e. for the same biceps input, it produced less supination motion. Whereas, location posterior center axis had the greatest mechanical advantage and produced the most motion out of all of the tendon locations. This lends further support for the importance of tendon wrapping.

In chronic or delayed cases of the ruptured distal biceps, tendon/muscle shortening and adhesion formation can make anatomic restoration of the tendon to the tuberosity difficult [53, 60]. For these cases, the surgeon must choose whether to attempt anatomic repair or to reconstruct the biceps tendon with a graft [35, 53, 60]. In our study, a proximal anatomic location represented the scenario where anatomic repair was chosen after the tendon was shortened due to retraction. The proximal anatomic location trended to have a lower moment arm than the native in all forearm positions, but was only significantly different in neutral. At this position, only part of the tendon wraps around the proximal half of the tuberosity not taking advantage of the full wrapping effect seen in the native case. However, this position could provide more wrapping of the tendon over the tuberosity than the anterior center axis location. Clinically these findings would suggest that if the muscle was contracted and the tendon could not be inserted to its native position then a proximal anatomic position would be better than a more central anterior one.

# 7.0 CONCLUSIONS AND FUTURE WORK

## 7.1 CONCLUSIONS

This biomechanical study provides support for the importance of anatomic restoration of the native tendon moment arm during the repair of ruptured distal biceps tendons. The surgeon needs to pay particular attention to the geometry of the tuberosity and be mindful of the location of tendon reattachment as it could play a critical role in maximizing the functional outcomes of patients. The study also provides data that shows supination strength testing at multiple positions throughout the range of motion might be required to evaluate the overall effectiveness of distal bicep tendon repair methods.

## 7.2 FUTURE WORK

Future work on this project will include a clinical follow up of patients who had a distal biceps repair and are more than two years post-operatively. Each patient will sign an IRB approved informed consent and complete a disabilities of the arm, shoulder, and hand (DASH) questionnaire. Upon completion of the follow-up appointment, patients will be given an honorarium for their participation. The medical records will be analyzed to assess co-morbidities. The patients' supination strength and endurance will be measured bilaterally using a custom made electronic testing apparatus, based on a patented hand strength testing device.

Strength data will be collected with the forearm placed in three positions: 60° pronated, neutral and 60° supinated.

The participants will then have a forearm, elbow, and wrist MRI scan. Using the MRI data, the tendon healing to cortical bone will be verified and its quality graded using a four-point ordinal scale by two blinded board certified radiologists. Additionally, the location, length, width and area of the bicep tendonous attachment will be determined using the MRI images. Finally, a biomechanical analysis based on the MRI imaging will be conducted to determine if the surgical reattachment location correlates to the stregth measures recorded.

# APPENDIX A

## IMAGE TO SPATIAL COORDINATES PROGRAM

```
%Program to convert Image Coordinates to MRI Spatial Coordinates
%Created by David M. Weir

clear all
home

%Cell Array of Image Data
data={
89.58   90.29   0.00     'Weir,David'    '09010512'  '02480000'  '61869628' ;
55.71   110.57  0.00     'Weir,David'    '09010512'  '02480000'  '61870236' ;
71.64   79.84   0.00     'Weir,David'    '09010512'  '02480000'  '61869740' ;
79.84   4.38    0.00     'Weir,David'    '09010512'  '02480000'  '61869740' ;
76.04   96.31   0.00     'Weir,David'    '09010512'  '02480000'  '61869532' ;
};

[r,s]=size(data);
n=1;

while n<=r

%Get image file information
name=data(n,4);
study_folder=datac;
seq_folder=data{n,6};
image_name=data{n,7};
image_file=fullfile(pwd,'DICOM',study_folder,seq_folder,image_name);

%Read in Dicom Info of image
dicom_info=dicominfo(image_file);

%Extract IOP from Dicom Attributes
T=dicom_info.ImagePositionPatient;
dir_cosines=dicom_info.ImageOrientationPatient;
x_cosines=dir_cosines(1:3,1);
y_cosines=dir_cosines(4:6,1);
z_cosines=cross(x_cosines,y_cosines);

%Build Transformation Matrix
transformation=vertcat(horzcat(x_cosines,y_cosines,z_cosines,T),[0,0,0,1]);
```

```
image_pts=[data{n,1},data{n,2},data{n,3},1]';

%Multiply points by transformation matrix
xyz_coords=transformation*image_pts;

xyz_data(n,1)=xyz_coords(1,1);
xyz_data(n,2)=xyz_coords(2,1);
xyz_data(n,3)=xyz_coords(3,1);

n=n+1;
end

%save
save('weir_keypts.txt','xyz_data','-ASCII')
```

## APPENDIX B

## MATLAB BICEPS MOMENT ARM SIMULATION CODE

```
%Distal Biceps Moment Arm Simulation Program
%Created by David M. Weir

%VARIABLE Description:

% AFR:              Unit vector along axis of forearm rotation corh to couh
% AFRv:             vector from corh to couh used for plotting
% C:                Direction Cosine Matrix
% I:                Index of maximum for angles array
% IC:               vector from insertion to contact point c1
% M_O:              Moment about the corh
% M_OB:             Moment about the AFR
% OC:               vector from tendon origin to contact point c1
% OCP:              vector from contact point c1 to origin_proj
% a:                row index of min of d
% angles:           array of angles between all possible combinations of
                    contact points
% b:                column index of min of d
% beta:             forearm angle counter for plots
% c1:               possible contact point 1
% c2:               possible contact point 2
% contact:          actual contact point
% contact_line:     line between c1 and c2
% corh:             center of radial head
% corh_original:    center of radial head before it was made (0,0,0)
% couh:             center of ulnar head
% curve_size:       number of control points on surface of proximal radius
% curves:           control points on surface of proximal radius
% curves_filename:  name of file with radius surface points
% d:                array of distances between the ins_pt and pts
% data:             xyz info of keypoints file
% data2:            data redefined with corh as origin
% data_size:        number of points in data
% f:                counter for while loop that ids Contour points of radius
                    at insertion slice
% force_direction:  unit vector from contact to tendon origin
% forearm_start_pos:position arm was scanned at
% g:                counter for while loop that ids Contour points of radius
                    at insertion slice
% heading:          plot heading text
% humerus:          line along humerus
% humerus_length:   length of humerus
```

```
% image_data:       array of pixel info from mri images
% increments:       amount of forearm rotation between MA calculation cycles
% ins_dir:          perpendicular vector from contact line to insertion
% ins_pt:           point chosen from imagin to represent insertion
% insertion:        closest control point to ins_pt
% insertion_image:  image that contains insertion
% j:                "angles" while loop counter
% k:                "angles" while loop counter
% key_points_filename: file name with keypoints data
% l:                number of rows in image data array
% lambda:           vector along AFR
% loa:              array with contact and origin pts
% m:                rows of pts array
% mesh_pts:         radius points for meshing
% n:                columns of pts array
% name:             name of patient
% normal:           normal unit vector of plane of rotated points
% option:           determines where to take ins_pt from
% orientation:      cosine of up_dir and ins_dir vectors
% origin:           bicep tendon origin
% origin_proj:      bicep tendon origin projected into insertion plane
% patient_last_name:last name of patient
% phi:              angle between contact point pairs
% pts:              points from insertion image
% q:                while loop counter to redefine curve points with corh as
origin
% r:                number of columns in image data
% rot_curves:       curve points rotated using C
% rot_mesh_pts:     mesh of rotated curve pts
% rot_pts:          points on insertion image rotated
% sim_name:         name for simulation file
% t:                vertices of triangles of mesh pts
% test:             determines whether a point is from the insertion image
% theta:            amount to rotate radius for it to be at -80
% up_dir:           perpendicular vector from contact line to origin
% v:                while loop counter for MA calculation cycle
% w:                while loop counter to redefine key points with corh as
origin
% wrap:             determines whether wrapping occured (1:Yes, 0:No)
% x:                x coordinate of key points
% x1:               min of M_OB
% x2:               max of M_OB
% y:                y coordinate of key points
% z:                z coordinate of key points
```

```
clear all
clc


image_data=load('weir_img_data.mat');

%Load Data (File must be in XYZ column format)
patient_last_name=input('Patient last name: ','s');
sim_name=input('Name of simulation: ','s');
key_points_filename=horzcat(patient_last_name,'_keypts.txt');
curves_filename=horzcat(patient_last_name,'_curve_data.txt');

data=load(key_points_filename);
data_size=size(data);

curves=load(curves_filename);
curve_size=size(curves);

%Estimation of Humerus Length
humerus_length=295;

%Center of radial head
corh=[data(1,1),data(1,2),data(1,3)] ;
corh_original=[data(1,1),data(1,2),data(1,3)] ;

%Redefine all points with corh as the origin

w=1;
while w<=data_size(1)
    data2(w,1)=data(w,1)-corh(1,1);
    data2(w,2)=data(w,2)-corh(1,2);
    data2(w,3)=data(w,3)-corh(1,3);
    w=w+1;
end

q=1;
while q<=curve_size(1)
    curves(q,1)=curves(q,1)-corh(1,1);
    curves(q,2)=curves(q,2)-corh(1,2);
    curves(q,3)=curves(q,3)-corh(1,3);
    q=q+1;
end

%Extract Components of Key Points
x=data2(:,1);
y=data2(:,2);
z=data2(:,3);

%Center of radial head (note: should be (0,0,0))
corh=[x(1,1),y(1,1),z(1,1)];

%Center of ulnar head
couh=[x(2,1),y(2,1),z(2,1)];
```

```
%Unit vector along axis of forearm rotation crh to cuh
AFR=(couh-corh)/norm((couh-corh));

%Origin of biceps

origin=data2(3,:)+(humerus_length*(data2(4,:)-data2(3,:))/norm(data2(4,:)-
data2(3,:)));

%Chosen Position of insertion on tuberosity ("ins_pt" from imaging)

option=input('Insertion Point from: 1)Key Points File or 2)Image : ');
if option ==1

    ins_pt=[x(5,1),y(5,1),z(5,1)];

    insertion_image=input('Name of Image with Insertion: ','s');
    name=image_data{1,4};
elseif option==2

    name=image_data{1,4};
    study_folder=image_data{1,5};
    seq_folder=image_data{1,6};
    image_name=input('Image Name: ','s');
    image_file=fullfile(pwd,'DICOM',study_folder,seq_folder,image_name);

    ins_image_coords=input('Input Image Coords of Insertion: ');

    dicom_info=dicominfo(image_file);

    T=dicom_info.ImagePositionPatient;
    dir_cosines=dicom_info.ImageOrientationPatient;
    x_cosines=dir_cosines(1:3,1);
    y_cosines=dir_cosines(4:6,1);
    z_cosines=cross(x_cosines,y_cosines);


transformation=vertcat(horzcat(x_cosines,y_cosines,z_cosines,T),[0,0,0,1]);


image_pts=[ins_image_coords(1,1),ins_image_coords(1,2),ins_image_coords(1,3),
1]';

    xyz_coords=transformation*image_pts;

    ins_pt(1,1)=xyz_coords(1,1)-corh_original(1,1);
    ins_pt(1,2)=xyz_coords(2,1)-corh_original(1,2);
    ins_pt(1,3)=xyz_coords(3,1)-corh_original(1,3);

    insertion_image=image_name;

end
```

```
%Contour points of radius at insertion slice

[l,r]=size(image_data);
f=1;
g=0;
while f<l
    test=strcmp(image_data{f,7},insertion_image);
    if test==1
        pts(g+1,1)=curves(f,1);
        pts(g+1,2)=curves(f,2);
        pts(g+1,3)=curves(f,3);

        g=g+1;
    end
     f=f+1;
end
[m,n]=size(pts);

AFRv=[x(2,1),y(2,1),z(2,1);x(1,1),y(1,1),z(1,1)];

%Find closest control point to chosen insertion point
q=1;

while q<=m
    d(q,1)=norm(ins_pt-pts(q,:));
    q=q+1;
end

[a,b]=min(d);

%Closest control point to ins_pt
insertion=pts(b,:);

[mesh_pts]=interpolate_pts(curves,m);


forearm_start_pos=-68; %from imaging
lambda=-1*[AFR(1);AFR(2);AFR(3)];
theta=(-80-forearm_start_pos)*pi/180;

v=1;
beta=-80;
while beta<=80

    %Elements of Direction Cosine Matrix
    C(1,1)=cos(theta)+lambda(1,1)^2*(1-cos(theta));
    C(1,2)=-lambda(3,1)*sin(theta)+lambda(1,1)*lambda(2,1)*(1-cos(theta));
    C(1,3)=lambda(2,1)*sin(theta) +lambda(3,1)*lambda(1,1)*(1-cos(theta));

    C(2,1)=lambda(3,1)*sin(theta) +lambda(1,1)*lambda(2,1)*(1-cos(theta));
    C(2,2)=cos(theta)+lambda(2,1)^2*(1-cos(theta));
    C(2,3)=-lambda(1,1)*sin(theta)+lambda(2,1)*lambda(3,1)*(1-cos(theta));

    C(3,1)=-lambda(2,1)*sin(theta)+lambda(3,1)*lambda(1,1)*(1-cos(theta));
```

```
    C(3,2)=lambda(1,1)*sin(theta) +lambda(2,1)*lambda(3,1)*(1-cos(theta));
    C(3,3)=cos(theta)+lambda(3,1)^2*(1-cos(theta));

    %Rotate contour points around AFR by amount theta
    rot_pts=(C*pts')';
    rot_curves=(C*curves')';
    rot_mesh_pts=(C*mesh_pts')';

    figure(v),

    %Plot rot_pts,original pts,insertion, and AFR


[t]=Delaunay2_5D(rot_mesh_pts);

trisurf(t,rot_mesh_pts(:,1),rot_mesh_pts(:,2),rot_mesh_pts(:,3),'facecolor','
w','edgecolor',[0,0,0])
hold on

    plot3(AFRv(:,1),AFRv(:,2),AFRv(:,3),'r-')

    %Plot line along humerus
    humerus=data2(3:4,:);

    %Find contact points (Defined as the two contour pts that make the
largest
    %angle with the origin of biceps

    k=1;
    angles=[0 0 0];
    [r,l]=size(angles);

    while k<=m;
        j=1;
        while j<=m;
            phi=acos(dot((rot_pts(k,:)-origin),(rot_pts(j,:)-
origin))/norm(rot_pts(k,:)-origin)/norm(rot_pts(j,:)-origin))*180/pi;

            angles(r,1)=k;
            angles(r,2)=j;
            angles(r,3)=phi;
            r=r+1;

            j=j+1;
        end

        k=k+1;
    end

    [phi,I] = max(angles(:,3));
    c1=rot_pts(angles(I,1),:);
    c2=rot_pts(angles(I,2),:);
    phi=angles(I,3);
    plot3(c1(1,1),c1(1,2),c1(1,3),'m.','MarkerSize',25')
```

```
    plot3(c2(1,1),c2(1,2),c2(1,3),'m.','MarkerSize',25')


    %Find  new location of insertion after rotation then plot
    insertion=rot_pts(b,:);
    plot3(insertion(1,1),insertion(1,2),insertion(1,3),'b.','MarkerSize',25)

    %Normal unit vector of plane of rotated points
    normal=cross(rot_pts(4,:)-rot_pts(1,:),rot_pts(2,:)-
rot_pts(1,:))/norm(cross(rot_pts(4,:)-rot_pts(1,:),rot_pts(2,:)-
rot_pts(1,:)));


    contact_line=(c2-c1)/norm(c2-c1);
    OC=origin-c1;
    origin_proj=(OC-dot(OC,normal)*normal)+c1;
    OCP=origin_proj-c1;
    IC=insertion-c1;

    %Find out whether wrapping occurs
    up_dir=origin_proj-((dot(OCP,contact_line)*contact_line)+c1);
    ins_dir=insertion-((dot(IC,contact_line)*contact_line)+c1);

    orientation=dot(up_dir,ins_dir)/norm(up_dir)/norm(ins_dir);

    if  -1.00001<=orientation & orientation<=-.99999
        wrap=1;
    else
        wrap=0;
    end

    %Determine contact point
    if v==1;
        if insertion==c2 | insertion==c1
            contact=insertion;

        else

            if .99999<=orientation & orientation<=1.00001
                contact=insertion;

            else
                if c1(1,2)<c2(1,2) %choose the more medial point
                    contact=c1;
                else
                    contact=c2;
                end
            end
        end

    else
        if insertion==c2 | insertion==c1
            if M_OB(v-1,3)==0
                contact=insertion;
```

```
            elseif M_OB(v-1,3)==1
                if c1(1,2)<c2(1,2) %choose the more medial point
                    contact=c1;

                else
                    contact=c2;

                end
            end
        else
            if .99999<=orientation & orientation<=1.00001

                if M_OB(v-1,3)==0 & sum(M_OB(:,3))==0
                    contact=insertion;

                else %M_OB(v-1,3)==1
                    if c1(1,2)<c2(1,2) %choose the more medial point
                        contact=c1;
                    else
                        contact=c2;
                    end

                end
            else
                if c1(1,2)<c2(1,2) %choose the more medial point
                    contact=c1;
                else
                    contact=c2;
                end
            end
        end
    end


    loa=vertcat(contact,origin);
    plot3(loa(:,1),loa(:,2),loa(:,3),'r','LineWidth',3)
xlim([-50 50]);
ylim([-50 50]);
xlim([-50 50]);
view([6 -90])
grid off
axis off
    %unit vector from contact to origin
    force_direction=(origin-contact)/norm(origin-contact);

    %Calculate Moment Arm
    M_O=cross(contact,force_direction);


    M_OB(v,1)=forearm_start_pos+(theta*180/pi);
    M_OB(v,2)=dot(M_O,AFR);
    M_OB(v,3)=wrap;
```

```
    %Amount to rotate around AFR
    increments=pi/18;
    theta=theta+increments;

    %figure heading
    heading=num2str(beta);
    beta=beta+10;
    title(heading);

    %Create new figure for every increment
    v=v+1;


end

figure(v),
x1=min(M_OB(:,1));
x2=max(M_OB(:,1));
plot(M_OB(:,1),M_OB(:,2))
hold on
plot(M_OB(:,1),M_OB(:,2),'+')
axis([x1 x2 0 20])

save(['C:\Documents and Settings\Dave\Desktop\Patient MRI
Scans\',name,'\',sim_name],'M_OB','-ASCII')
```

## APPENDIX C

## ELBOW SIMULATOR CONTROLLER PROGRAM

```
PROGRAM

'Program 0

'TODO: edit your program here


'////////////////////////////////////////////////////////////////////////

' Variable Initialization


' Number of Array Variables

Dim SA(2)


'Array Variable Length

Dim SA0(700)

Dim SA1(700)


'Number of Scalar Variables

Dim SV(11)
```

```
'ADC - Analog to Digital Inputs On
ADC ON

'////////////////////////////////////////////////////////////////////////
' Sampling Setup

'Sampling Variable Initializations
Samp Clear

'A - Load Cell Biceps Force
Samp0 SRC P6472
Samp0 Base SA0

'B - Biceps Reference
Samp1 SRC SV1
Samp1 Base SA1

'Sampling Period (Milliseconds)
P6915 = 50

'////////////////////////////////////////////////////////////////////////
' CPU Period Setup
Period 0.001
```

```
'////////////////////////////////////////////////////////////////////////
' Acceleration Levels
Jog Acc X3000
Jog Dec X3000

'////////////////////////////////////////////////////////////////////////
' Counter Initialization
SV0 = 1

'////////////////////////////////////////////////////////////////////////
' Pattern for Control Values

'  1 = Reference
'  2 = Current State
'  3 = Error Signal
'  4 = Previous Error
'  5 = Control Signal
'  6 = Previous Control Signal
'  7 = Proportional Gain
'  8 = Integral Gain
'  9 = Derivative Gain
' 10 = 2x Previous Error
```

```
'////////////////////////////////////////////////////////////////////////

'Biceps Force Values (X - Axis)


SV1 = 1

SV2 = SV1

SV3 = 0

SV4 = 0

SV5 = 0

SV6 = 0

SV7 = 0.2

SV8 = 0

SV9 = 0

SV10 = 0


'////////////////////////////////////////////////////////////////////////

'Start Sampling

Set 105


'////////////////////////////////////////////////////////////////////////

'Jog Velocities Zero

P12348 = 0
```

```
'////////////////////////////////////////////////////////////////////////

'Control Loop

While (SV0 < 800)


'////////////////////////////////////////////////////////////////////////

'Reference Load

        If (SV0 <= 100)

                SV1 =1

        Else If (SV0 <= 700)

                SV1 = 1+14*SIN((SV0-100)/600*180)

        Else

                SV1 = 1

        EndIf


'////////////////////////////////////////////////////////////////////////

' Biceps Load Control

                SV2 = P6472

                SV3 = SV2 - SV1

                SV5 = SV6 + (SV7 + SV8 + SV9) * SV3 - (SV7 + 2 * SV9) * SV4 + (SV9) *
SV10


                If (SV5 < 0)

                        Clr 796
```

```
            Set 797
        Else
            Clr 797
            Set 796
        EndIf

        P12348 = Absf(SV5)

        SV10 = SV4
        SV4 = SV3
        SV6 = SV5

' Pause
    DWL 0.02

' Counter Increment
    SV0 = SV0 + 1

Wend

'Stop Movement
P12348 = 0
Clr 796
```

```
Clr 797
'Stop Sampling
INH -105
ENDP
```

# APPENDIX D

## DATA ACQUISITION MATLAB CODE

```
%Sensor DAQ Program
%Created by David M. Weir

clear all
home

%Channel 0: Potentiometer
%Channel 2: Biceps Load Cell
%Channel 3: Torque Sensor

filename=input('Enter a name for test file: ','s');

%Potentiometer Configuration

pot_ref_1= 3.3896;              %Voltage output in position #1
pos_1=0;                        %Position #1 [deg]
pot_ref_2= 4.2767;              %Voltage output in position #2
pos_2=-63.0 ;                   %Position #2 [deg]

pot_scaling=(pos_1-pos_2)/(pot_ref_1-pot_ref_2)
pot_offset=(pos_1-(pot_scaling*pot_ref_1))

%Biceps Load Cell Configuration

ref_load_1=0;
loadcell_volt_1=1.2136;
ref_load_2=10.35;
loadcell_volt_2=1.8803;

load_scaling= (ref_load_1-ref_load_2)/(loadcell_volt_1-loadcell_volt_2)
load_offset= (ref_load_1-(load_scaling*loadcell_volt_1))
%%
%Torque Sensor
%Low In 00.000  Low Rd 000.00
%High In 20.088 High Rd 050.00
ref_torque_1=-25;
sensor_volt_1=0;
ref_torque_2=25;
sensor_volt_2=10; %Should be 10!!!!!!
```

```
torque_scaling= abs((ref_torque_1-ref_torque_2)/(sensor_volt_1-
sensor_volt_2))
%%

%DAQ Settings
AI = analoginput('nidaq','Dev1');
set(AI,'InputType','Differential')
chan1 = addchannel(AI,0);        % Add first 3 channels
chan2 = addchannel(AI,2);
chan3 = addchannel(AI,3);
duration = 30;                  % 30 second acquisition
set(AI,'SampleRate',100)
ActualRate = get(AI,'SampleRate');
set(AI,'SamplesPerTrigger',(duration*ActualRate)+1)
AI.ChannelskewMode = 'Min';
%%

%Establish figure before DAQ starts
figure
set(gcf,'doublebuffer','on') %Reduce plot flicker

subplot(3,1,1);
title('Position')
axis([0 duration -90 90])

subplot(3,1,2);
title('Biceps Load')
axis([0 duration 0 25])

subplot(3,1,3);
title('Forearm Torque')
axis([0 duration -5 5])

disp('Press enter to start data acquisition')
pause

start(AI)
j = 1;

while AI.SamplesAcquired < AI.SamplesPerTrigger
    while AI.SamplesAcquired < ((ActualRate*j)+1)
    end
    preview = peekdata(AI,((ActualRate*j)+1));
    x=(0:1/ActualRate:j)';

    position_peek=pot_scaling*preview(:,1)+pot_offset;

    subplot(3,1,1); plot(x,position_peek)
    axis([0 duration -90 90])
    title('Position')
    drawnow

    load_peek=load_scaling*preview(:,2)+load_offset;
```

```
    subplot(3,1,2); plot(x,load_peek)
    axis([0 duration 0 25])
    title('Biceps Load')
    drawnow

    torque_peek=torque_scaling*(preview(:,3)-5);

    subplot(3,1,3); plot(x,torque_peek)
    axis([0 duration -5 5])
    title('Forearm Torque')
    drawnow

    j = j + 1;
end

[voltage,time]=getdata(AI);

potentiometer_voltage=voltage(:,1);
biceps_loadcell_voltage=voltage(:,2);
torque_sensor_voltage=voltage(:,3);

position=pot_scaling*voltage(:,1)+pot_offset;
biceps_load=load_scaling*voltage(:,2)+load_offset;
torque=torque_scaling*(voltage(:,3)-5);

data=horzcat(time,voltage,position,biceps_load,torque);

save(['C:\Documents and Settings\Dave\Desktop\Biceps Biomech
Study\',filename],'data','-ASCII')
```

## APPENDIX E

## CODE FOR FILTERING DATA IN MATLAB

```
%Program to Filter Data
%Created by David M. Weir

clear all
home

files={

     'Intact_1.xls'    'Intact_60S_15lb_1.txt'  '60S'   'A3';
     'Intact_1.xls'    'Intact_60S_15lb_2.txt'  '60S'   'D3';
     'Intact_1.xls'    'Intact_60S_15lb_3.txt'  '60S'   'G3';
     'Intact_1.xls'    'Intact_N_15lb_1.txt'     'N'   'A3';
     'Intact_1.xls'    'Intact_N_15lb_2.txt'     'N'   'D3';
     'Intact_1.xls'    'Intact_N_15lb_3.txt'     'N'   'G3';
     'Intact_1.xls'    'Intact_60P_15lb_1.txt'  '60P'   'A3';
     'Intact_1.xls'    'Intact_60P_15lb_2.txt'  '60P'   'D3';
     'Intact_1.xls'    'Intact_60P_15lb_3.txt'  '60P'   'G3'
    }

[r,s]=size(files);
v=1;
while v<=r
spreadsheet_name=files(v,1);
filename=files(v,2);
worksheet_name=files(v,3);
paste_spot=files(v,4);
data=load(filename{1});

time=data(:,1);
voltage=data(:,2:4);

[b,a]=butter(5,1/50,'low');
[c,d]=butter(2,.8/50,'low');
position=flipud(filter(b,a,flipud(filter(b,a,data(:,5)))));
biceps_load=flipud(filter(b,a,flipud(filter(b,a,data(:,6)))));
torque=flipud(filter(c,d,flipud(filter(c,d,data(:,7)))));

figure(1),
plot(time,data(:,6))
ylim([0 20])
```

```
hold on
plot(time,biceps_load,'r')
ylim([0 20])

figure(2),
plot(time,data(:,7))
ylim([-5 5])

hold on
plot(time,torque,'r')
ylim([-5 5])
xlim([0 max(time)])

figure(3),
plot(biceps_load,torque)
ylim([-5 5])
xlim([0 20])

[Y,I]=max(biceps_load);
p2=I;
while Y>=1 & I>0
    I=I-1;
    if I>0
        Y=biceps_load(I);
    end
end
p1=I+1;

[slope,slope_int,residuals,rint,stats]=regress(torque(p1:p2),biceps_load(p1:p
2));

filtered_data=horzcat(time(p1:p2),biceps_load(p1:p2),torque(p1:p2));
xlswrite(spreadsheet_name{1},filtered_data,worksheet_name{1}, paste_spot{1});


summary(1,1)=(slope);
summary(1,2)=(slope_int(1));
summary(1,3)=(slope_int(2));
summary(1,4)=(stats(1));

paste_spot2=horzcat('B',num2str(v));
xlswrite(spreadsheet_name{1},summary,'Moment Arm Summary', paste_spot2);

v=v+1;
end
```

# APPENDIX F

## RESULTS SUMMARY

| | **60° Supination** | **0° Neutral** | **60° Pronation** |
|---|---|---|---|
| | *avg. ±stdev (mm)* | *avg. ±stdev (mm)* | *avg. ±stdev (mm)* |
| **Native** | 5.67 ±2.86 | 10.44 ±1.45 | 8.04 ±1.25 |
| **Anatomic** | 6.24 ±3.30 | 10.41 ±2.03 | 8.41 ±1.22 |
| **Anterior Center Axis** | 0.15 ±3.48 | 7.66 ±1.95 | 8.26 ±1.88 |
| **Posterior Center Axis** | 7.21 ±3.02 | 9.93 ±0.93 | 8.69 ±0.76 |
| **Proximal Anatomic** | 4.69 ±2.75 | 8.83 ±2.06 | 7.56 ±1.60 |

| | **5-lb** | **10-lb** | **15-lb** |
|---|---|---|---|
| | *avg. ±stdev (deg)* | *avg. ±stdev (deg)* | *avg. ±stdev (deg)* |
| **Native** | 68° ±9° | 71° ±9° | 73° ±10° |
| **Anatomic** | 70° ±10° | 74° ±10° | 75° ±11° |
| **Anterior Center Axis** | 59° ±17° | 62° ±16° | 62° ±15° |
| **Posterior Center Axis** | 74° ±8° | 78° ±8° | 80° ±8° |
| **Proximal Anatomic** | 68° ±11° | 71° ±10° | 73° ±9° |

# BIBLIOGRAPHY


1. Chillemi, C., M. Marinelli, and V. De Cupis, *Rupture of the distal biceps brachii tendon: conservative treatment versus anatomic reinsertion--clinical and radiological evaluation after 2 years.* Arch Orthop Trauma Surg, 2007. **127**(8): p. 705-8.

2. Hetsroni, I., et al., *Avulsion of the distal biceps brachii tendon in middle-aged population: is surgical repair advisable? A comparative study of 22 patients treated with either nonoperative management or early anatomical repair.* Injury, 2008. **39**(7): p. 753-60.

3. Baker, B.E. and D. Bierwagen, *Rupture of the distal tendon of the biceps brachii. Operative versus non-operative treatment.* J Bone Joint Surg Am, 1985. **67**(3): p. 414-7.

4. Norman, W. 1999.

5. Mrabet, Y. 2008.

6. Neumann, D.A., *Kinesiology of the Musculoskeletal System*. 1st ed. 2002, St. Louis: Mosby Inc.

7. Biodex Medical Systems, I., *Biodex Multi Joint-System Pro: Setup and Operation Manual*. 2006, Shirley, New York.

8. *The Color Atlas of Human Anatomy*, ed. V. Vannini and G. Pogliani, New York: Harmony Books.

9. Forthman, C.L., et al., *Cross-sectional anatomy of the bicipital tuberosity and biceps brachii tendon insertion: relevance to anatomic tendon repair.* J Shoulder Elbow Surg, 2008. **17**(3): p. 522-6.

10. Safran, M.R. and S.M. Graham, *Distal biceps tendon ruptures: incidence, demographics, and the effect of smoking.* Clin Orthop Relat Res, 2002(404): p. 275-83.

11. Leighton, M.M., C.A. Bush-Joseph, and B.R. Bach, Jr., *Distal biceps brachii repair. Results in dominant and nondominant extremities.* Clin Orthop Relat Res, 1995(317): p. 114-21.

12. Morrey, B.F., et al., *Rupture of the distal tendon of the biceps brachii. A biomechanical study.* J Bone Joint Surg Am, 1985. **67**(3): p. 418-21.

13. eORTHOPOD. 2003.

14. O'Driscoll, S.W., L.B. Goncalves, and P. Dietz, *The hook test for distal biceps tendon avulsion.* Am J Sports Med, 2007. **35**(11): p. 1865-9.

15. Seiler III, J.G., et al., *The Distal Biceps Tendon - Two potential mechanisms involved in its rupture: Arterial supply and mechanical impingement.* J Shoulder Elbow Surg, 1995. **4**: p. 149-56.

16. Dobbie, R.P., *Avulsion of the Lower Biceps Brachii Tendon, Analysis of Fifty-one Previously Unreported Cases.* Am. J. Surg., 1941. **51**: p. 662-683.

17. Meherin, J.M. and E.S.K. Jr., *The Treatment of Ruptures of the Distal Biceps Brachii Tendon.* Am. J. Surg., 1960. **99**: p. 636-640.

18. Boyd, J.B. and L.D. Anderson, *A Method for the Reinsertion of the Distal Biceps Tendon.* J Bone Joint Surg Am, 1961. **43**: p. 1041-1043.

19. Le Huec, J.C., et al., *Distal rupture of the tendon of biceps brachii. Evaluation by MRI and the results of repair.* J Bone Joint Surg Br, 1996. **78**(5): p. 767-70.

20. Klonz, A., et al., *Rupture of the distal biceps brachii tendon: isokinetic power analysis and complications after anatomic reinsertion compared with fixation to the brachialis muscle.* J Shoulder Elbow Surg, 2003. **12**(6): p. 607-11.

21. Agins, H.J., et al., *Rupture of the distal insertion of the biceps brachii tendon.* Clin Orthop Relat Res, 1988(234): p. 34-8.

22. Failla, J.M., et al., *Proximal radioulnar synostosis after repair of distal biceps brachii rupture by the two-incision technique. Report of four cases.* Clin Orthop Relat Res, 1990(253): p. 133-6.

23. Davison, B.L., W.D. Engber, and L.J. Tigert, *Long term evaluation of repaired distal biceps brachii tendon ruptures.* Clin Orthop Relat Res, 1996(333): p. 186-91.

24. Karunakar, M.A., P. Cha, and P.J. Stern, *Distal biceps ruptures. A followup of Boyd and Anderson repair.* Clin Orthop Relat Res, 1999(363): p. 100-7.

25. Kelly, E.W., B.F. Morrey, and S.W. O'Driscoll, *Complications of repair of the distal biceps tendon with the modified two-incision technique.* J Bone Joint Surg Am, 2000. **82-A**(11): p. 1575-81.

26. Bisson, L., et al., *Complications associated with repair of a distal biceps rupture using the modified two-incision technique.* J Shoulder Elbow Surg, 2008. **17**(1 Suppl): p. 67S-71S.

27. Barnes, S.J., S.G. Coleman, and D. Gilpin, *Repair of avulsed insertion of biceps. A new technique in four cases.* J Bone Joint Surg Br, 1993. **75**(6): p. 938-9.

28. Balabaud, L., et al., *Repair of distal biceps tendon ruptures using a suture anchor and an anterior approach.* J Hand Surg [Br], 2004. **29**(2): p. 178-82.

29. Khan, A.D., et al., *Repair of distal biceps tendon ruptures using suture anchors through a single anterior incision.* Arthroscopy, 2008. **24**(1): p. 39-45.

30. Strauch, R.J. and M.P. Rosenwasser, *Single incision repair of distal biceps tendon rupture.* Tech Hand Up Extrem Surg, 1998. **2**(4): p. 253-61.

31. Lynch, S.A., D.M. Beard, and P.A. Renstrom, *Repair of distal biceps tendon rupture with suture anchors.* Knee Surg Sports Traumatol Arthrosc, 1999. **7**(2): p. 125-31.

32. Pinto, M.C., D.S. Louis, and L.J. PJ, *Distal biceps tendon repair: a single incision technique.* Tech Hand Up Extrem Surg, 2000. **4**(1): p. 30-3.

33. Bain, G.I., et al., *Repair of distal biceps tendon rupture: a new technique using the Endobutton.* J Shoulder Elbow Surg, 2000. **9**(2): p. 120-6.

34. Greenberg, J.A., et al., *EndoButton-assisted repair of distal biceps tendon ruptures.* J Shoulder Elbow Surg, 2003. **12**(5): p. 484-90.

35. Hallam, P. and G.I. Bain, *Repair of chronic distal biceps tendon ruptures using autologous hamstring graft and the Endobutton.* J Shoulder Elbow Surg, 2004. **13**(6): p. 648-51.

36. Sharma, S. and G. MacKay, *Endoscopic repair of distal biceps tendon using an EndoButton.* Arthroscopy, 2005. **21**(7): p. 897.

37. Ranelle, R.G., *Use of the Endobutton in repair of the distal biceps brachii tendon.* Proc (Bayl Univ Med Cent), 2007. **20**(3): p. 235-6.

38. Pereira, D.S., et al., *Surgical repair of distal biceps tendon ruptures: a biomechanical comparison of two techniques.* Am J Sports Med, 2002. **30**(3): p. 432-6.

39. Lemos, S.E., E. Ebramzedeh, and R.S. Kvitne, *A new technique: in vitro suture anchor fixation has superior yield strength to bone tunnel fixation for distal biceps tendon repair.* Am J Sports Med, 2004. **32**(2): p. 406-10.

40. Idler, C.S., et al., *Distal biceps tendon repair: a biomechanical comparison of intact tendon and 2 repair techniques.* Am J Sports Med, 2006. **34**(6): p. 968-74.

41. Spang, J.T., P.S. Weinhold, and S.G. Karas, *A biomechanical comparison of EndoButton versus suture anchor repair of distal biceps tendon injuries.* J Shoulder Elbow Surg, 2006. **15**(4): p. 509-14.

42. Kettler, M., et al., *Failure strengths in distal biceps tendon repair.* Am J Sports Med, 2007. **35**(9): p. 1544-8.

43. Mazzocca, A.D., et al., *Biomechanical evaluation of 4 techniques of distal biceps brachii tendon repair.* Am J Sports Med, 2007. **35**(2): p. 252-8.

44. Kettler, M., et al., *Reattachment of the distal tendon of biceps: factors affecting the failure strength of the repair.* J Bone Joint Surg Br, 2008. **90**(1): p. 103-6.

45. Murray, W.M., S.L. Delp, and T.S. Buchanan, *Variation of muscle moment arms with elbow and forearm position.* J Biomech, 1995. **28**(5): p. 513-25.

46. Haugstvedt, J.R., R.A. Berger, and L.J. Berglund, *A mechanical study of the moment-forces of the supinators and pronators of the forearm.* Acta Orthop Scand, 2001. **72**(6): p. 629-34.

47. Henry, J., et al., *Biomechanical analysis of distal biceps tendon repair methods.* Am J Sports Med, 2007. **35**(11): p. 1950-4.

48. Giuffre, B.M. and M.J. Moss, *Optimal positioning for MRI of the distal biceps brachii tendon: flexed abducted supinated view.* AJR Am J Roentgenol, 2004. **182**(4): p. 944-6.

49. Kaeding, C., R. Fischer, and T. Anderson, *Modified distal biceps tendon repair.* J Orthop Tech, 1996. **4**: p. 29-32.

50. Gallagher, M.A., et al., *Effects of age, testing speed, and arm dominance on isokinetic strength of the elbow.* J Shoulder Elbow Surg, 1997. **6**(4): p. 340-6.

51. D'Arco, P., et al., *Clinical, functional, and radiographic assessments of the conventional and modified Boyd-Anderson surgical procedures for repair of distal biceps tendon ruptures.* Am J Sports Med, 1998. **26**(2): p. 254-61.

52. Moosmayer, S., A. Odinsson, and I. Holm, *Distal biceps tendon rupture operated on with the Boyd-Anderson technique: follow-up of 9 patients with isokinetic examination after 1 year.* Acta Orthop Scand, 2000. **71**(4): p. 399-402.

53. Wiley, W.B., et al., *Late reconstruction of chronic distal biceps tendon ruptures with a semitendinosus autograft technique.* J Shoulder Elbow Surg, 2006. **15**(4): p. 440-4.

54. Weinstein, D.M., et al., *Elbow function after repair of the distal biceps brachii tendon with a two-incision approach.* J Shoulder Elbow Surg, 2008. **17**(1 Suppl): p. 82S-86S.

55. De Carli, A., et al., *Surgical repair of the distal biceps brachii tendon: clinical and isokinetic long-term follow-up.* Knee Surg Sports Traumatol Arthrosc, 2009. **17**(7): p. 850-6.

56. Nesterenko, S., et al., *Elbow strength and endurance in patients with a ruptured distal biceps tendon.* J Shoulder Elbow Surg, 2009.

57. Peeters, T., et al., *Functional outcome after repair of distal biceps tendon ruptures using the endobutton technique.* J Shoulder Elbow Surg, 2009. **18**(2): p. 283-7.

58. Cheung, E.V., M. Lazarus, and M. Taranta, *Immediate range of motion after distal biceps tendon repair.* J Shoulder Elbow Surg, 2005. **14**(5): p. 516-8.

59. McKee, M.D., et al., *Patient-oriented functional outcome after repair of distal biceps tendon ruptures using a single-incision technique.* J Shoulder Elbow Surg, 2005. **14**(3): p. 302-6.

60. Darlis, N.A. and D.G. Sotereanos, *Distal biceps tendon reconstruction in chronic ruptures.* J Shoulder Elbow Surg, 2006. **15**(5): p. 614-9.

61. Freeman, C.R., et al., *Nonoperative treatment of distal biceps tendon ruptures compared with a historical control group.* J Bone Joint Surg Am, 2009. **91**(10): p. 2329-34.